Understanding and Tuning the Electrical Conductivity of Activated Carbon: A State-of-the-Art Review

Adrián Barroso Bogeat

Published online: 07 Oct 2019.

Submit your article to this journal ↗

View related articles ↗

View Crossmark data ↗

Taylor & Francis
Taylor & Francis Group

Check for updates

REVIEW

Understanding and Tuning the Electrical Conductivity of Activated Carbon: A State-of-the-Art Review

Adrián Barroso Bogeat[a,b] (iD)

aDepartamento de Ciencia de los Materiales e Ingeniería Metalúrgica y Química Inorgánica, Universidad de Cádiz, Puerto Real, Cádiz, Spain; bInstituto de Investigación en Microscopía Electrónica y Materiales (IMEYMAT), Universidad de Cádiz, Puerto Real, Cádiz, Spain

ABSTRACT

During the last decades, there has been a growing interest and research activity in the use of activated carbon (AC) and related materials as electrodes in electrochemical energy conversion and storage devices, like fuel cells, supercapacitors, and lithium-ion batteries. Among other factors, electrical properties, and especially conductivity, are well-known to play a pivotal role on the performance of ACs in these devices. Furthermore, other novel applications of AC-based materials, such as in electroadsorption, electrocatalysis, sensors and actuators, and so on, also rely heavily on their unique electrical properties. Therefore, the knowledge, understanding, and rationalization of these properties are essential with a view to assessing many of the current and future technological applications of ACs. The present paper critically reviews the available literature, including the latest published reports, on the electrical conductivity of AC. The accurate measurement of this property for ACs is rather difficult and requires the application of low to moderate compression to ensure the electrical contact. Estimated conductivity values are the result of a complex combination between a number of factors, among which the intrinsic conductivity of the single particles, their degree of contact and packing should be highlighted. Intrinsic conductivity is mainly determined by the texture, surface chemistry, and graphitization degree of AC, which strongly depend on the feedstock and the preparation method. Thus, the influence of these factors on the electrical conductivity of the resulting ACs is examined. Moreover, the influence of different adsorbed chemical species, mainly oxygen and water, is also dealt with. On the other hand, special emphasis is paid to the temperature dependence of conductivity, as its analysis is a powerful tool to gain insight into the electronic band structure and electron conduction process in carbon materials. In this regard, the different proposed mechanisms for electrical conduction in AC are exposed and compared.

Table of contents

1. Introduction

Activated carbon (AC, henceforward) is a general term commonly applied to a wide family of essentially amorphous carbon materials characterized by its excellent and unique textural properties (i.e., specific surface area, porosity, and pore size distribution) and surface chemical features. It is well-established that these properties and features of ACs and related materials strongly depend on the feedstock and the method employed in their preparation process, embracing the activating agent as well as the operational conditions.[1–5] Currently, ACs are manufactured on a large scale from a great variety of precursors with high carbon content and low amount of inorganic compounds, including woods, coals, lignite, peat, petroleum coke, coconut shell, nutshell, almond shell, corncob, sugarcane bagasse, vine shoots, fruit stones, polymers, and so on.[1–3,6–10] Due to the growing awareness on the control of environmental pollution, nowadays the production of AC materials from both industrial and agricultural waste products has become a topic of increasing research interest and activity, with a view not only to their controlled removal and valorization but also to prepare lower cost ACs.[5,8,11] Anyway, the use of a given raw material is largely conditioned by its availability and economic cost, although it also depends on the specific applications of the resulting AC and the manufacture installation.[2]

ACs and AC-based materials are broadly employed in a number of environmental and industrial applications, such as drinking and wastewater treatment, separation and storage of gases and vapors, removal of organic and inorganic pollutants by adsorption both from liquid and gaseous effluents, solvent and automotive/gasoline recovery, in heterogeneous catalysis either as catalysts on their own or more frequently as catalyst supports, in electrocatalysis, sensors and actuators, and so forth.[1–3,12]

Over the last few decades, special attention has been paid to the use of ACs as electrode materials in devices devoted to electrochemical energy storage and conversion, mainly supercapacitors,[13–23] lithium and sodium-ion batteries,[24–31] and fuel cells.[32–38] Amongst other factors, such as specific surface area, pore size distribution, chemical and thermal stability, presence of electroactive surface functional groups and structures, electrolytes, and so on,[5,19,22,39,40] electrical conductivity is generally agreed to play a pivotal role on the suitability and performance of ACs and related materials as electrode components in the aforementioned devices.[41,42] On the other hand, the properties of the carbon support, especially its electrical conductivity, largely determine the electrochemical performance of carbon-based electrocatalysts.[43,44] Therefore, it becomes evident that the assessment, knowledge, understanding, and rationalization of the electrical properties, especially conductivity, are critical in order to develop and prepare AC-based materials satisfying the operational requirements and showing excellent performances in many of their current and future technological applications, particularly those concerning electrochemical energy storage and conversion. Thus, the present paper is intended to critically review the available literature on the electrical properties of AC materials, with particular attention to conductivity, covering from the first studies conducted at the beginning of the 20th century to the latest published reports. The review is divided into several sections and subsections, encompassing a detailed description of the experimental setups employed to measure the electrical conductivity of granular and powder ACs, a comprehensive discussion of the major factors affecting the intrinsic conductivity of these carbon materials (i.e., texture, surface chemistry, and graphitization degree), the effects of adsorption of gases and vapors on the conductivity, as well as the temperature dependence of this property, which allows gaining some insight into the dominant electron conduction mechanisms in ACs and related materials.

Before going into details, there are some basic concepts which will be handled throughout the paper, so that it is worth clarifying them in advance. Electrical resistivity (ρ, in $\Omega \cdot m$) is an intrinsic property that quantifies how strongly a given material opposes to the flow of electric current. From a mathematical point of view, it is defined as the ratio of the electric field (E, in $V \cdot m^{-1}$) inside a material to the density of the current (J, in $A \cdot m^{-2}$) that it creates:

$$\rho = \frac{E}{J} \tag{1}$$

The above is a basic and general definition, which can be also expressed as follows for materials having a uniform cross section:

$$\rho = R \cdot \frac{A}{l} \tag{2}$$

where R is the electrical resistance of the material, and l and A denote the length and the cross sectional area of the piece of the material, respectively. Such a way

of defining resistivity makes it an intrinsic property, that is, a property of a material or system which is independent on both its mass and geometrical form.

Electrical conductivity (σ, in $\Omega^{-1} \cdot m^{-1}$ or $S \cdot m^{-1}$) is defined as the reciprocal of electrical resistivity, so that it is also an intrinsic property that measures the ability of a given material to conduct an electric current.

$$\sigma = \frac{1}{\rho} = \frac{1}{E} \tag{3}$$

Because of the simple and direct relationship existing between electrical resistivity and conductivity, both terms will be indistinctly used throughout the present paper. Furthermore, the electrical conductivity of semiconductors, such as carbon materials, is well-known to broadly vary as a result of the exposure of the material to specific frequencies of light. For this reason, and following the indications of Kuriyama and Dresselhaus in their earlier work, the terms intrinsic electrical conductivity or resistivity will be employed when referring to the conductivity or resistivity in the absence of light,[45] unless the opposite is clearly stated.

2. Measuring the electrical conductivity of activated carbons and related materials

Since the earlier studies conducted by Skaupy and Kantorowicz on metal powders in the 1930's,[46,47] the measurement of the electrical conductivity has been widely applied as a simple, fast, and low cost technique for characterizing granular, powder, and porous materials, including a variety of carbonaceous materials.[48–56] Nonetheless, these experiments entail some theoretical and practical problems, which are briefly dealt with below.

According to the contact theory formulated by Mrozowski and Holm in the 1950's, the electrical conductivity of a granular or powdered carbon material, such as AC, depends not only on the interparticle separation distance,[51,53,57–60] but also on the average particle size, as well as on the chemical nature of the carbon surface. In this regard, the separation of the contribution of particle cores and surfaces to the bulk conductivity of several powder samples was methodically analyzed by Braun and Herger.[61]

Electron tunneling, which involves the ability of electrons to jump across the gaps and voids between closely spaced grains and particles,[62,63] has been regarded as the dominant electrical transport mechanism in granular and powder carbon-based materials. Obviously, the narrowing of gaps and the increasing contact between grains and particles should result in a notable enhancement in the bulk electrical conductivity of the sample. In this connection, the number of contacts established between neighboring particles is a pivotal factor, since it ultimately determines the number of paths or channels available for the effective electron transport.[62] Several theoretical studies devoted to estimate the mean number of contacts (i.e., the degree of contact) during compaction between identical spherical particles in a random packing, or in the more complex case of a mixture of various proportions of spherical particles having two different diameters, have been reported in the literature.[64–68] However, the average number of contacts is almost impossible to determine for real granular and powdered materials, essentially due to the grains and particles exhibit simultaneously a broad distribution of sizes and a strongly variable morphology,[54] which even may undergo modifications during compaction.

Therefore, measuring the electrical conductivity of particulate carbons, such as ACs, typically requires applying a pressure or range of pressures to a packed bed of the carbon material, whose height or length and electrical resistivity decrease with increasing applied pressure until a plateau is finally reached. At this point, the electrical resistance associated with contact between particles is overcome and, after correcting for the empty bed values, the measured resistances can be considered as the real resistance values, from which the electrical conductivities are easily derived by simply applying the following expression, resulting from the combination of Equations (2) and (3)[49,56,63,69]:

$$\sigma = \frac{l}{R \cdot A} \tag{4}$$

where l is the distance between the two plungers in the compression chamber in m, R denotes the measured electrical resistance in Ω, and A stands for the area of the plunger surface in m^2.

As far as the contact resistances for a column of a particulate material are concerned, it should be pointed out that they come from two different origins, tunneling and constriction.[54] The tunneling resistances may reach very high values, being especially relevant for metallic particles coated by thin oxide layers and almost negligible for simply ground carbon materials without any additional surface treatment. By contrast, constriction resistances are related with the narrowness of the conducting path as a result of the small contact area between two particles or grains. The mathematical expression for the constriction resistance is only well-established for the ideal situation of two spheres forming an elastic contact.[70] Nevertheless, real

situations are considerably more complicated, since the actual geometry of the contacts is poorly defined in powdered and granular materials, owing to their rough surfaces and to the fact that any contact usually consists of a number of touching points rather than of a well-defined surface.[54]

On the other hand, the inelastic and/or plastic deformations of the grains and particles frequently occurring during compaction when measuring the electrical resistance of a granular or powdered material should be also taken into account. The origin of such deformations is connected with the highly heterogeneous distribution of internal forces within packings,[59,71–73] thus resulting in a network of grains and particles bearing most of the applied pressure. Even though this network steadily grows and ramifies with increasing compaction, a number of non-constrained particles and grains still remain. Consequently, the grains and particles are deformed in a very irregular way, so that the contact areas may strongly vary throughout the packed column. This complex problem is exacerbated by the density inhomogeneities arising from the friction forces established between neighboring particles and against the inner walls of the sample holder. As a result, the mean coordination number for each grain or particle depends on its position within the packed column, and hence the total electrical resistance of the granular or powdered sample is a function of both the geometry (i.e., length and diameter) of the holder as well as of the ratio of the average particle or grain size to the inner diameter of the holder. Finally, some additional difficulties, such as crumbling, crushing, and breaking of grains and particles because of the applied compacting pressure, should be also worth mentioning.[54]

In view of the several hindrances and difficulties discussed above, it becomes evident that the problem of the electrical resistivity/conductivity of a granular or powdered material is unsolvable in an exact way from the theoretical point of view. Notwithstanding, a few models, which assume a number of simplifications, assumptions, and approximations, have been proposed to describe these heterogeneous media, such as those derived from the percolation theory and effective media theories. A detailed and comprehensive discussion of these theories and their applications to carbon-based materials is out of scope of the present review, and can be found elsewhere.[54,58,74] Just as a brief summary, it should be pointed out that above the percolation threshold the electrical conductivity (σ) of a compacted granular or powdered carbon material comprising gas-filled voids may be described as:

$$\sigma = \sigma_h \left(\frac{\Phi - \Phi_c}{1 - \Phi_c} \right)^{t'} \quad (5)$$

where σ_h is the intrinsic conductivity of the carbon material, Φ its volume fraction, Φ_c the percolation threshold, and t' stands for an exponent related with both the percolation threshold and the shape of the grains and particles.[43,54] As an illustrative example, Figure 1 depicts the electrical conductivities as a function of the volume fractions of grains and particles for a variety of carbonaceous materials, including both natural and artificial graphite, several activated carbons, a commercial carbon black, and cokes. The solid lines were calculated by applying Equation (5) to the experimental data, Φ and Φ_c being estimated by the following equations:[54]\

$$\Phi = \frac{d}{d_g} \quad (6)$$

$$\Phi_c = \frac{d_p}{d_g} \quad (7)$$

where d represents the apparent density of the carbon material undergoing compaction, d_p is its apparent density in the non-compacted state, and d_g stands for the apparent density of the particles and grains. From this figure it becomes evident that for graphite materials, labeled as NG and AG in the plot, conductivity is relatively high even at low volume fractions, while the opposite applies to carbon black (CB) and pinewood-derived activated carbon (AC). Finally, for carbon powders showing a large anisometry degree (i.e., coconut
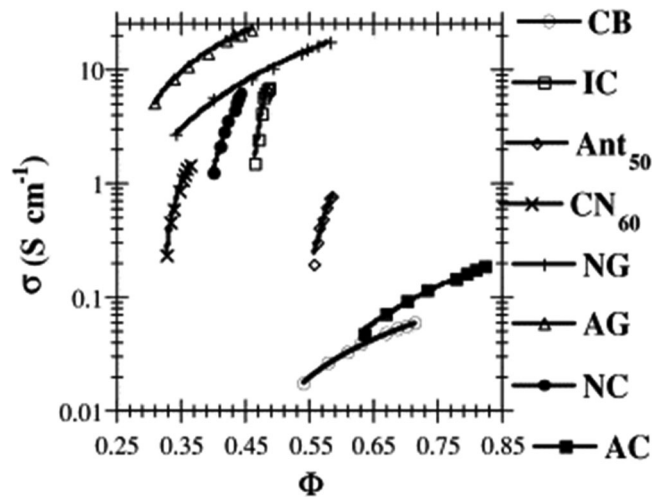
Figure 1. Electrical conductivity (σ) as a function of volume fraction (Φ) for a variety of carbonaceous materials. Caption: CB, carbon black; IC, isotropic coke; Ant50, Anthracite activated at 50% burn-off; CN_{60}, coconut shell-derived activated carbon; NG, natural graphite; AG, artificial graphite; NC, needle coke; AC, pinewood-derived activated carbon. Reprinted from Celzard et al.,[54] with permission from Elsevier.
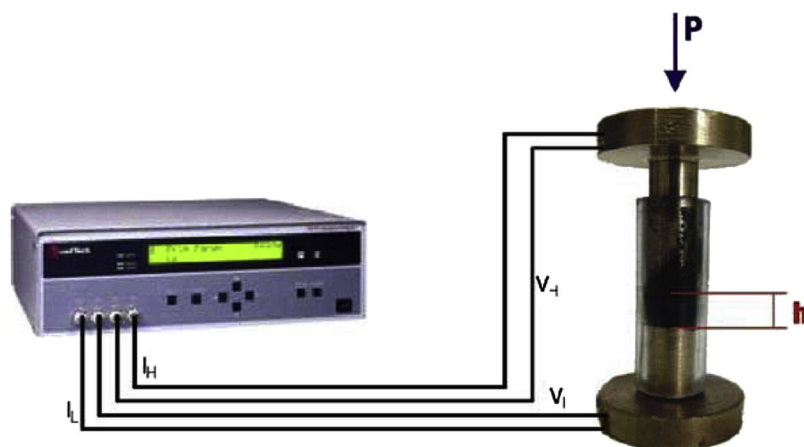
Figure 2. Compression chamber or sample holder typically employed for measuring the electrical conductivity of granular and powdered carbon materials under moderate compression. Reprinted from Barroso-Bogeat et al.,[69] with permission from Elsevier.

shell-based activated carbon, CN_{60}, and needle coke, NC), conductivity at low volume fractions drops below their corresponding intrinsic values, but it sharply increases when applying modest compression pressures.[43]

Most of the experimental setups employed for measuring the electrical resistivity/conductivity of granular and powdered carbon materials are commonly based on the original design first reported by Brodd and Kosawa,[75] and the further modifications subsequently introduced by Espinola et al.[52] Specifically, the most frequent device consists of a hollow thick-walled cylinder constructed with a non-conducting material, namely a ceramic or a plastic like polyvinyl chloride (PVC), into which the carbon material is poured and then compressed between two close-fitting metallic plungers or pistons forming the electrodes, the bottom one fixed and the upper one movable.[52,54,62,63,69,76] This compression chamber or sample holder is illustrated in Figure 2. Such an apparatus ensures that the number of grains or particles contained in a column of a few centimeters of the carbon material amounts a minimum quantitative in order to obtain both reproducible and representative resistivity/conductivity values.[54]

The compression of the carbonaceous sample is achieved by applying different loads, as a rule in the range from some hundreds of kPa up to some MPa, on the upper piston either by placing several weights[54,62] or with the aid of a universal testing machine,[63,69,76] as shown in Figure 3. In this regard, it is worth mentioning that the lowest applied pressure should be enough to get a good electrical contact between the sample particles or grains and the plungers, while the highest one should be low enough to avoid the crumbling, crushing, and breaking of the particles or grains. Under these conditions, the increase in the volume fraction of particles as a consequence of their spatial rearrangement would be the only expected effect of compaction.[54,63]

Concerning the measurement of the dc electrical conductivity/resistivity of the compressed carbon material, two closely related methods have been traditionally employed: the two-probe method and the four-probe method, which are schematically illustrated in Figure 4. In the former, a voltage is applied so that a known current is forced to flow through the sample (in one direction then in the opposite one), which is placed between the two probes fitted into the two pistons. Then, the resulting voltage drop is recorded at the same points by using a potentiometer, thus allowing calculating the conductivity of the carbon material from its resistivity as usual.[54,56,77] On the contrary, the latter method is an electrical impedance measuring technique that uses separate pairs of current-carrying and voltage-sensing electrodes in order to make much more accurate measurements as compared to the simpler two-probe method.[51,63,77,78] Separation of current and voltage electrodes enables to suppress contact resistances and thereby measuring low resistance values, typically below 100 Ω, in a precise manner.[79] This four-probe method is usually preferred to its two-probe counterpart chiefly because this latter provides results which are strongly sensitive to the gap existing between the probes inserted into the granular or powdered carbon sample column.[54,76]

At this point, it is worth mentioning that, irrespective of the applied measurement method and prior to performing the experiments, the resistance of the metallic pistons should be verified to be much lower than those measured for the carbon materials under study. Moreover, several current values should be also tested for each sample in order to ensure that conduction is purely ohmic in nature.[54,63]
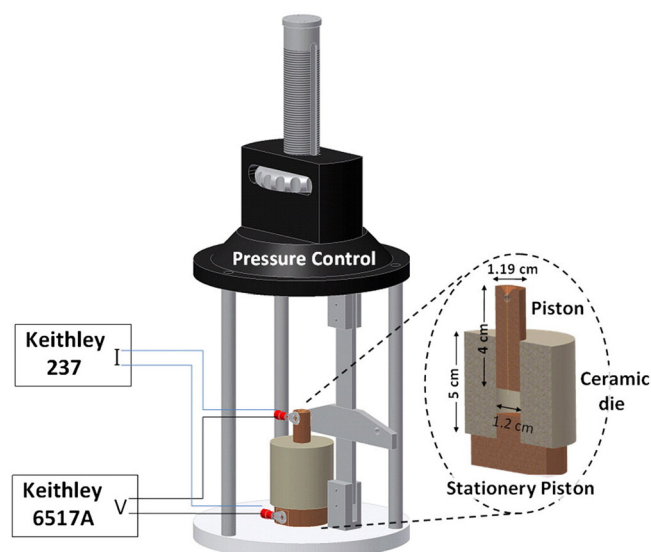
Figure 3. Experimental assembly for measuring the electrical conductivity of granular and powdered carbon materials under moderate compression. Note how in this case the different loads to achieve the compression of the carbonaceous sample are applied to the upper piston by using a universal testing machine. Reprinted from Marinho et al.,[55] with permission from Elsevier.
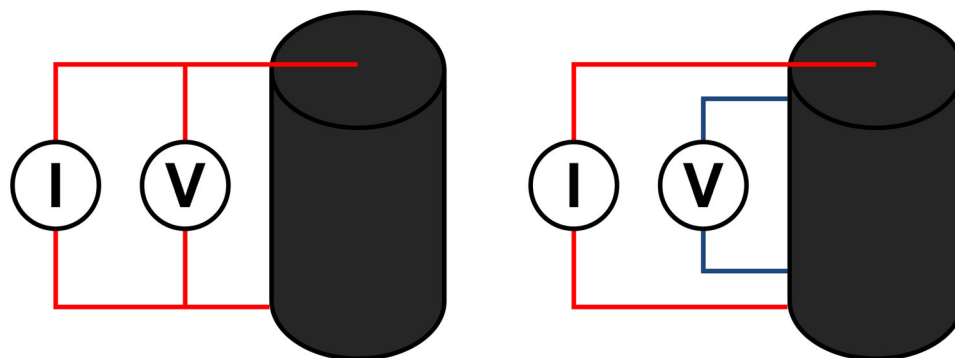
Figure 4. Schematic representation of the two probe (left) and four probe (right) methods typically employed for measuring the electrical resistivity/conductivity of compressed carbon materials. V and I represent a voltmeter and an ammeter, respectively.

Finally, it should be highlighted that the above-described experimental setup has been also employed to measure the temperature-dependent electrical conductivity of AC materials.[80,81] For such an aim, the compression chamber containing the carbon sample under a given pressure is introduced inside an oven. A thermocouple with the hot junction as close as possible to the carbonaceous material is employed to accurately monitor its temperature.

3. Influence of different factors affecting the intrinsic or intraparticle electrical conductivity of activated carbons and related materials

It is well-established that the *overall* electrical conductivity (herein referred to those conductivity values estimated from experimental measurements under moderate compression) of ACs and other granular and powdered carbonaceous materials depends on the *intrinsic* conductivity of the single carbon particles (also commonly referred to as *intraparticle* conductivity in the literature), the resistance of the contacts between them, as well as the volume density of the latter.[43] Although the overall electrical conductivity of compressed AC materials is determined to a large extent by the contact resistance, the intrinsic conductivity of the grains also shows a significant contribution. Therefore, the present section is aimed at comprehensively discussing the influence of the main factors affecting the intrinsic conductivity of AC's particles: texture, surface chemistry, and graphitization degree.

3.1. Influence of texture

Among the variety of factors affecting the intrinsic or intraparticle electrical conductivity of ACs and related

materials, the influence of texture could be considered as the simplest one and thereby the best understood and interpreted. In this regard, a number of papers focused on the effect of textural features of AC-based materials, resulting from the application of different preparation methods, activating agents, and operational conditions, have been published in the last decades. At this point, it should be kept in mind that the control of the texture of ACs has been traditionally accomplished by changing the preparation method (i.e., physical and chemical activation, or their combination) and operational conditions (e.g., carbonization and activation temperature and time, feedstock to chemical activating agent ratio, and so forth). However, these changes in the textural features are very frequently accompanied by notable modifications in other properties of the resulting ACs, such as the graphitization degree and particularly the surface chemistry. Even for a series of ACs prepared from the same precursor material, by using the same method and showing markedly different textural features, the intrinsic conductivity values may not be directly comparable due to strong differences both in the concentration and nature of their surface functional groups and structures, as well as in their graphitization degree. More realistically, in these cases the observed variations in the intrinsic conductivity will be the consequence of the complex interplay between the changes involving also the chemical surface features and the graphitization degree.

Despite all the above, it is generally accepted that the intrinsic electrical conductivity of granular and powder carbon materials is largely a function of the matter-free space existing in their constituent particles and grains. Obviously, such space comprises the porosity corresponding to the intraparticle voids.[5,62] In principle, the correlation is rather simple: the larger the total pore volume of the AC sample, the lower its intrinsic electrical conductivity. Such a dependence was clearly evidenced by Hernández et al. for heat-treated coals and Eucalyptus char,[82] and by Emmerich et al. for Babassu nut-derived chars.[83] Similar results were subsequently reported by Barroso-Bogeat et al. for a couple of carbonized samples prepared by pyrolysis of vine shoots at 600 and 900 °C under nitrogen atmosphere.[5] Both chars were essentially macroporous solids and the total pore volume dropped from $0.62 \, cm^3 \cdot g^{-1}$ to $0.46 \, cm^3 \cdot g^{-1}$ as the carbonization temperature rose from 600 to 900 °C due to pore shrinkage, thus resulting in an enhancement of electrical conductivity of up to three orders of magnitude. These authors also studied the effect of three different activating agents (i.e., air, carbon dioxide, and steam)

on the intrinsic electrical conductivity of ACs prepared from the above carbonized samples by physical activation. They attempted to correlate the experimental variations in conductivity with the textural data; nonetheless, neither the extent of the specific surface area nor the porosity of the ACs was the predominant factors determining the magnitude of their electrical conductivity. In stark contrast, the porosity development was much larger for AC samples prepared from vine shoots by chemical activation with phosphoric acid, zinc chloride, and potassium hydroxide, thus leading to lower conductivity values as compared to their physically activated counterparts. Moreover, in this case an excellent correlation between the variation sequences for electrical conductivity and total pore volume was reported.

3.2. Influence of surface chemistry

The chemical nature of the surface of ACs and related materials is well-known to depend on both the starting precursor materials and the methods employed in their preparation, as well as on whether they are subsequently purposely modified or not. Surface chemistry significantly influences the adsorptive, electrical, electrochemical, catalytic, acid-base, redox, hydrophilic-hydrophobic, and other properties of ACs, which accounts for the growing interest and attention by many researchers.[1,3,6,84–87] The reactivity of AC materials at low temperature is specifically connected with the chemical nature of their surfaces as this factor controls the inherently associated surface chemistry. This latter term refers to unpaired electrons and to the type, quantity, and bonding of different heteroatoms, especially oxygen and nitrogen to a lesser extent, which are bonded to carbon atoms at the edges of graphene sheets forming a variety of surface functional groups and structures. Such carbon-heteroatom surface groups are considered to be identical to those typically found and described in aromatic organic compounds, thereby reacting in a similar way with many chemical reagents and being then strongly differentiated in terms of their chemical reactivity. The following sections are devoted to critically review the available literature concerning the influence on electrical conductivity of different functional groups and structures frequently found on AC surface, with special emphasis on those containing oxygen and nitrogen.

3.2.1. Influence of oxygen-containing surface functional groups and structures

Oxygen surface groups of ACs are usually classified into acidic groups (i.e., carboxyl groups, anhydrides,
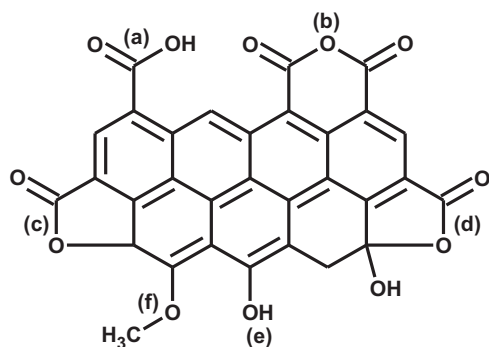
Figure 5. Oxygen functional groups and structures on AC surface featuring acidic character: (a) carboxylic acid, (b) carboxylic anhydride, (c) lactone, (d) lactol, (e) phenol, and (f) ether (this latter is considered either as a neutral or weakly acidic functionality by several authors[88])

Figure 6. Oxygen functional groups and structures on AC surface featuring basic character: (a) pyrone, (b) chromene, and (c) quinone.

hydroxyls, lactones, lactol, and phenol groups), basic groups (i.e., pyrone, chromene, quinones, and carbonyl groups), and neutral groups (i.e., ether groups).[88–93] Furthermore, AC materials owe a reducing ability to oxygen functional groups such as phenol, lactone, carbonyl, and quinone.[94] Oxygen surface groups may be also involved in electrostatic interactions and form chelate complexes.[95] As a summary, Figures 5 and 6 gather the variety of oxygen-containing surface functional groups and structures typically found in AC materials, which are classified according to their acid-base character.

Since in typical ACs oxygen is nearly ubiquitously found and is by far the most abundant heteroatom, there is a general trend aimed at tailoring the surface chemistry of these carbon materials by incorporating or removing oxygen functional groups. In this regard, an assortment of techniques and methods has been widely applied to increase or decrease the content of oxygen surface groups. ACs have been oxidized by using a variety of chemical agents in either a gaseous or a liquid phase.[96–99] Among the broad series of available oxidants, nitric acid in aqueous solution can be probably considered as the most frequently employed.[100–103] Other common oxidizing agents are air, oxygen, ozone, nitric oxides, sulfuric acid, hydrogen peroxide, potassium permanganate, and sodium and ammonium peroxydisulphates.[104] The heterogeneous reactions between the gaseous or liquid phase and the AC surface are performed under different heating temperatures and using solutions of varying concentration and pH, depending on the desired effects. As a rule, the higher the temperature and the stronger the oxidant, the larger the extent of the AC surface oxidation is.[105] Gas-phase oxidation at low temperatures often leads to formation of strong acidic groups (e.g., carboxylic), while various oxygen-

containing functional groups are formed at higher temperatures with a predominant population of weakly acidic groups, such as phenols.[87,104,106] On the contrary, liquid-phase oxidation is considerably more complex and can introduce a higher amount of oxygen functionalities onto the carbon surface at much lower temperatures as compared to the gas-phase oxidation, thus resulting in more severe modifications in the AC surface chemistry.[104,106] It is generally agreed that oxidation in liquid phase with strong oxidizing agents like nitric acid, nitric and sulfuric acids mixture, and sodium peroxydisulphate gives rise to ACs with predominance of carboxylic groups,[91,101,105,107–109] whereas wet oxidation treatment with hydrogen peroxide brings about an increase in the surface concentration of phenol groups.[104] Finally, it should be highlighted that liquid-phase oxidation may be severely detrimental to the texture of AC.[100,110] In fact, it has been reported that strong oxidation, as that carried out with concentrated nitric acid at its boiling point, can even completely destroy the carbon structure, leading to some kind of water-soluble humic substance.[104]
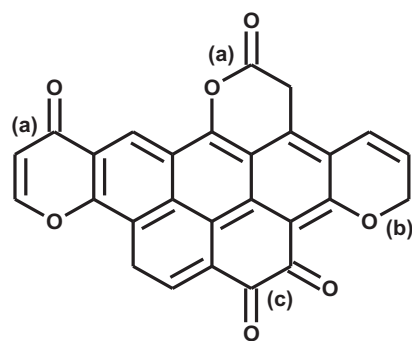
Most of the oxygen-containing functional groups and structures can be removed from the AC surface by heat treatment at high temperature (i.e., above 700 °C) under inert atmosphere (e.g., nitrogen, argon or helium). As a result of this thermal treatment, particular surface functionalities decompose at different characteristic temperatures with release mainly of carbon oxides as well as of other minor heteroatom-containing gases, such as nitrogen oxides, ammonia, and hydrogen sulfide.[6,104,111,112] Figure 7 summarizes the temperature ranges reported in the literature for the thermal decomposition of the major oxygen functional groups and structures typically found on AC surface.

The thermal decomposition of oxygen functional groups gives rise to the creation of active sites at the

Figure 7. Temperature ranges reported in the literature for the thermal decomposition of different oxygen-containing functional groups and structures typically found on AC surface [109] (references therein): (a) carboxylic acid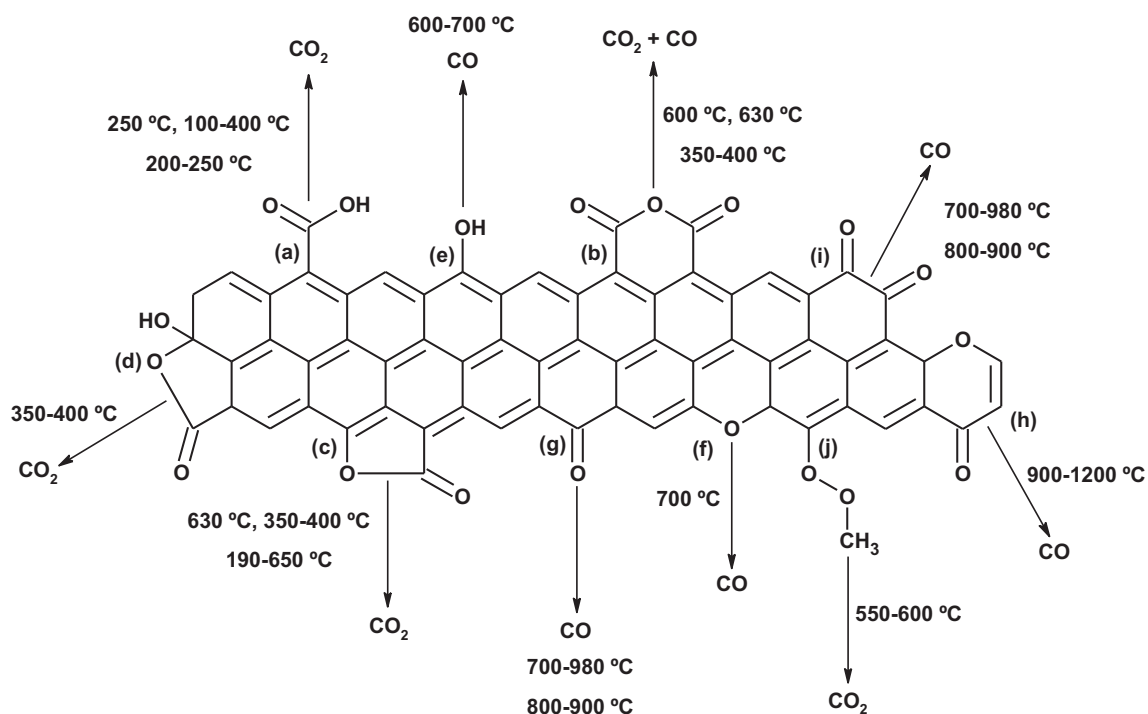, (b) carboxylic anhydride, (c) lactone, (d) lactol, (e) phenol, (f) ether, (g) carbonyl, (h) pyrone, (i) quinone, and (j) peroxide. Adapted from Figueiredo et al.,[109] with permission from Elsevier.

edges of the graphene sheets and thereby to an increase both in the basicity[104,108] and hydrophobicity[113–115] of the carbon surface. Nevertheless, such changes in the surface chemical nature are not stable because the aforesaid highly reactive carbon sites favor oxygen readsorption and formation of new acidic functional groups upon exposure to oxygen or air.[114,116,117] Therefore, heat treatment under hydrogen atmosphere at temperatures above 800 °C is usually preferred as it produces a highly stable carbon surface. In addition to the removal of surface oxygen complexes, this effect has been also associated with the stabilization of some reactive sites by involving them in carbon-hydrogen bonds and/or with the gasification of the loosely bound and most reactive unsaturated carbon atoms from the edges of graphene layers.[104,113,114,117] The basicity of the resulting heat-treated AC samples arises from the oxygen-free Lewis basic sites on the graphene sheets, on the one hand, and from the few oxygen-containing structures (i.e., pyrone and chromene) which remains in the carbon surface, on the other.[118,119]

The effect of oxygen chemisorption on the electrical conductivity of AC materials was first explored superficially by Smeltzer and McIntosh in the early 1950's.[120] They reported that the resistance of AC rods was increased by chemisorption of oxygen, this increase being greater with higher oxidation degrees. It was postulated that the formation of functional groups and structures on AC surface through the reaction of electronegative oxygen with electron donating carbon atoms located on the edge of the nanographene sheets causes a certain localization of the conduction electrons and, thereby, an increase in electrical resistance. However, it remained an open question whether these variations of resistance with oxygen chemisorption are accounted for by changes in electron mobility, in the thermal activation energy for electronic conduction or by the introduction or removal of electron traps.[121]

After these initial and promising results, the investigation of the influence of surface chemistry, and especially of oxygen-containing complexes, on the electrical properties of ACs almost fell into oblivion for the next 30 years. Thus, the first attempt to systematically study the effect of oxygen surface functional groups and structures was conducted by Barton and Koresh in the 1980's.[121] In their work, the electronic properties of a commercial carbon cloth activated by thermal treatment in air at 400 °C, by oxidation with an aqueous solution of nitric acid, and by a combination of these two treatments were determined and tentatively correlated with both the pore structure and surface oxide concentration of the

resulting materials. The aforesaid activation methods were selected in order to ensure the preparation of AC cloths (ACCs, hereafter) with broadly varied total oxygen contents. In this regard, the latter was expected to be higher for the sample activated with air and then subjected to treatment with refluxing nitric acid, and lower for that thermally activated in air. The ACC prepared by chemical activation with nitric acid should have a total oxygen content intermediate between those of the two previous samples. The electrical resistance at room temperature was measured for the as-prepared ACCs and after their heat treatment at increasing temperatures up to 900 °C in inert atmosphere. The resistance of the pristine carbon cloth, taken as reference, was found to be very low and remained nearly unaltered after the thermal treatments at several temperatures. In stark contrast, the variation of resistance with heat treatment temperature for the ACCs was markedly different. The resistance of the sample activated with air at 400 °C was almost constant until a heating temperature of 400 °C was attained, and then it dropped sharply with increasing temperature. For both carbon samples prepared by oxidation with nitric acid the resistance fell by about four orders of magnitude as heat treatment temperature increased from room temperature up to 900 °C. These resistance changes were ascribed to the progressive thermal decomposition of particular carbon-oxygen surface functionalities during the heat treatment of the ACCs under inert atmosphere. As previously discussed in the present section and reported by a number of works, such surface oxygen complexes decompose thermally at different characteristic temperatures (cf. Figure 7) with release of gases, mainly water, carbon monoxide and carbon dioxide.[6,109,111,112,122] From the results obtained in this work, the existence of some influence of the concentration of oxygen-containing surface functional groups and structures on the electronic properties of the ACCs appeared to be clearly evidenced. Furthermore, the resistance measurements also corroborated the expected sequence for the oxidizing power of the three employed activation treatments and hence for the total oxygen content of the prepared ACC samples.

The previous work was further complemented by Polovina et al., who oxidized a lab-made and cellulose-based ACC by treatments with a wide series of chemical agents, including air, nitric acid, hydrogen peroxide, and iron (III) nitrate, and attempted to correlate both the amount and type of oxygen surface structures with the electrical resistance measurements for the resulting oxidized carbon products.[123] Similarly to the earlier results reported by Barton and Koresh,[121] the pristine ACC exhibited the lower resistance and higher conductivity, while for the oxidized ACCs the measured values were extremely different and ranged from about 500 Ω for the sample oxidized with hydrogen peroxide to about 30,000 Ω for that prepared by oxidation with iron (III) nitrate. Obviously, this overall increase in resistance for the oxidized samples as compared to the raw ACC was largely ascribed to the formation of surface oxygen complexes during the oxidative treatments, with the consequent increasing localization of the electrons in the conduction band of the carbon material. Both the non-oxidized and oxidized ACC samples were submitted to heat treatment at several temperatures up to 850 °C under inert atmosphere, in order to assess the influence of the thermal decomposition of the different types of surface oxygen groups formed on the electrical resistance. For all the samples, the resistance variation below 200 °C was quite similar (i.e., the slope of the resistance versus heat treatment temperature plot was roughly the same) and mostly associated with the loss of hygroscopic water. Above such temperature, the following major changes were noted. The resistance was found to decrease steadily in the 420–850 °C range for the sample oxidized with air and over the whole temperature range for that oxidized with iron (III) nitrate. Stepwise changes in the 250–600 °C and 600–850 °C intervals were observed for the sample prepared by oxidizing treatment with nitric acid. By contrast, both the non-oxidized and hydrogen peroxide-oxidized samples showed only small resistance changes. Moreover, it should be pointed out that the resistance values after the heat treatment at the maximum temperature (i.e., 850 °C) were similar for all the oxidized ACCs and somewhat higher than for the raw ACC, thus confirming that the thermal decomposition of the surface oxides was not complete at 850 °C. On the basis of the above results, it was concluded that the total amount of oxygen groups formed on the ACC surface after the application of the different oxidation procedures varied in the following order: iron (III) nitrate > nitric acid > air > hydrogen peroxide.

These two latter works clearly evidenced that electrical resistance measurements are a simple and reliable method which can be applied to obtain a qualitative assessment of surface oxygen complexes in AC-based materials, as well as for comparison of the effect of different oxidizing agents and treatments.

Barroso-Bogeat et al. have also explored the influence of the surface chemical features on the intrinsic electrical conductivity for a broadly varied series of ACs prepared

from vine shoots by physical activation with air, carbon dioxide, and steam, as well as by chemical activation with phosphoric acid, zinc chloride, and potassium hydroxide.[5] For both groups of samples the presence of oxygen-containing complexes on carbon surface was found to have a significant and detrimental effect on their conductivity values, being much more pronounced for those ACs prepared by physical activation. Specifically, as evidenced by FT-IR spectroscopy and Boehm titration the ability of the three activating agents to promote the formation of oxygen surface functional groups and structures in the carbonized samples during the physical activation stage was higher in the following order: air ≫ carbon dioxide > steam, which was well in agreement with the variation sequence observed for the electrical conductivity of such AC materials. As far as the chemically activated samples are concerned, their intrinsic conductivity values were strongly influenced by the presence of heteroatoms coming from the activating agent, particularly phosphorus. In this regard, phosphorus-containing groups and structures on AC surface increase electronic localization and disrupt the π-conjugation, with the concomitant increase in electrical resistance. A more detailed discussion of the influence of phosphorus on the electrical behavior of AC-based materials will be presented in later paragraphs.

The role of surface oxygen functional groups on the electrical resistivity was also investigated for AC fiber cloths (ACFCs, henceforth) by Hashisho et al., with a view to optimizing the suitability and energy efficiency of the direct electrothermal regeneration of these carbon adsorbents after the adsorption of volatile organic compounds (VOCs) from gaseous streams.[124] Four virgin commercial ACFC samples with selected activation levels and specific surface area values ranging from 849 to 1,763 $m^2 \cdot g^{-1}$ were treated with a 1/1 (v/v) mixture of concentrated nitric and sulfuric acids for 5 days and with pure hydrogen at 950 °C for 3 h in order to change the density of their oxygen functional groups. In line with previously reported results,[125] the resistivity increased with activation degree both for the virgin and chemically-treated ACFCs. Such trend was mainly ascribed to the larger porosity development as well as to the lower graphitization degree of the carbon samples with increasing activation levels. As expected, hydrogen treatment led to a modest reduction in the resistivity and oxygen content of the pristine ACFC, whereas both parameters markedly increased by one to two orders of magnitude after acid treatment, regardless of the activation degree. These observed changes in resistivity with acid treatment were interpreted on the

basis that the main barrier to electron conduction is supposed to be located at the graphitic crystallite boundaries, whose oxidation produces an increase in the band gap with the consequent reduction in the number of available electrons in the conduction band of the carbon material. Obviously, the effect caused by the hydrogen treatment was fairly the opposite, thus decreasing the band gap and resistivity of the raw ACFC samples.

3.2.2. Influence of nitrogen-containing surface functional groups and structures

After oxygen, which is ubiquitously found in ACs, nitrogen is considered to be the second most abundant heteroatom in these carbon materials. Nonetheless, in stark contrast to oxygen complexes, nitrogen-containing surface functional groups and structures are not formed spontaneously on AC surface upon exposure to air,[87,104] essentially because of the much lower reactivity of the nitrogen molecule as compared to the oxygen one. As a consequence, the total amount of nitrogen in carbonaceous materials is usually negligible and mostly attributable to the presence of this element in the precursor material. In spite of the typically low nitrogen content of AC materials, this heteroatom can be easily introduced in the carbon matrix by two strategies: (i) reaction of the previously prepared AC with nitrogen-containing reagents, including ammonia, urea, melamine, and hydrogen cyanide, or (ii) preparation of the AC from either a nitrogen-rich organic compounds, such as carbazole, some polymers (e.g., polyacrylonitrile, polyaniline or polypyrrole), acridine, and so on, or mixtures of nitrogen-containing precursors with nitrogen-free materials.[87,104,126]

Similarly to oxygen, incorporation of nitrogen into the carbon matrix can be accomplished from either a gas or a liquid phase by means of nitrogen-containing reagents.[104] Ammonia is by far the most common gaseous source of nitrogen, being frequently used at temperatures ranging from 400 to 1,000 °C.[127] Concerning the liquid phase modification, carbon samples, either pre-oxidized or not, are usually impregnated with aqueous or alcoholic solutions of the nitrogen-containing compounds, such as carbazole, nitrogen-enriched polymers, acridine, melamine or urea, and subsequently subjected to a heat treatment at temperatures comprised between 400 and 1,020 °C.[128,129] In this connection, it is worth highlighting that pre-oxidation of carbons, especially chars with low graphitization degrees, leads to the formation of chemical bonds between the carbon surface and the basic
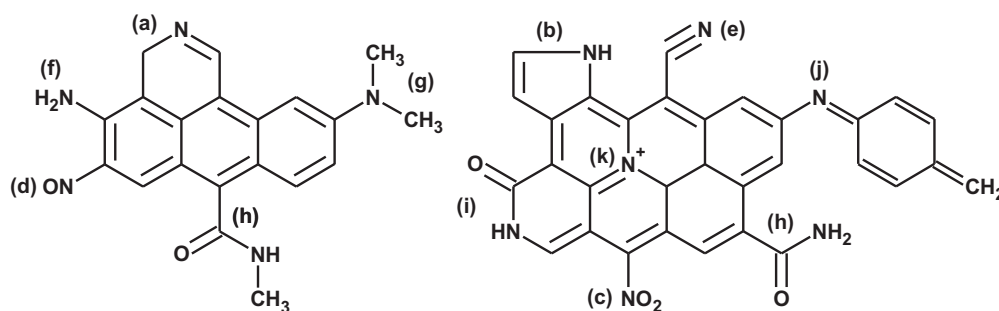
Figure 8. Nitrogen functional groups and structures on AC surface: (a) pyridine, (b) pyrrole, (c) nitro, (d) nitroso, (e) nitrile, (f) primary amine, (g) tertiary amine, (h) primary (right) and secondary (left) amide, (i) lactam, (j) imine, (k) quaternary amine.

nitrogen-containing reagent, thus resulting in carbon materials featuring enhanced total nitrogen contents.[130–132]

It is well-established that both the amount and type of the different nitrogen complexes present on the surface of AC materials strongly depend on the applied treatment, including factors such as the nitrogen-containing reagent, the chemical reactivity of the carbon surface, and the heat treatment temperature.[104,133] This latter parameter largely determines the nitrogen chemistry on ACs surface, since some nitrogen functional groups and structures are thermally unstable at high temperatures, thus decomposing with evolution mainly of nitrogen oxides and other minor nitrogen gaseous species. The variety of nitrogen surface functionalities that can be formed on ACs surface are schematically compiled in Figure 8. According to several works, lactam and imide structures are chiefly obtained by amination with ammonia, whereas amide groups are formed by ammoxidation with an ammonia-oxygen gaseous mixture. Additionally, all these structures can be easily transformed into pyrrole and pyridine by heat treatment at appropriate temperatures.[104,133–135] Interconversion of nitrogen functionalities is also possible; for example, amides have been reported to convert into lactams and nitriles.[133]

In a similar way to oxygen, nitrogen surface functional groups and structures are also well-known to markedly influence the acid-base character of AC materials, which is ultimately governed by the degree of heterogeneity of the aforesaid functionalities.[136] Heat treatment of AC surface with nitrogen-containing reagents at low and moderate temperatures (i.e., below 530 °C) mainly yields lactam, imide, and amine structures, which are slightly acidic in nature. On the contrary, heat treatment at high temperatures leads to the formation of quaternary nitrogen (i.e., nitrogen atoms with sp^2 hybridization occupying the position of carbon atoms in graphene layers), pyridine, and pyrrole structures,[127] these two latter conferring basic features to the carbon material.

The presence of nitrogen in the carbon matrix is generally agreed to play a pivotal role not only on the performance of AC-based materials in adsorptive[126,132,136–149] and catalytic[126,150–158] applications, but also on their electrical properties, including conductivity.[126,154] Nevertheless, the effect of nitrogen doping on electrical conductivity of ACs and other carbon-based materials is still far from clarified, thus being a topic of intense discussion. In this regard, at least three basic questions should be addressed in order to understand and rationalize the above-mentioned effect: (i) what type of conductivity is promoted in nitrogen-doped ACs, (ii) what types of nitrogen-containing functionalities influence the electrical conductivity of these carbon materials, and (iii) how conductivity of nitrogen-doped ACs varies with nitrogen content.[154] The most recent works and advances aimed at solving these complex questions are briefly summarized below.

As previously pointed out in above paragraphs and shown in Figure 8, nitrogen is able to occupy several sites and get involved in a variety of functional groups and structures upon its incorporation to the carbon matrix of ACs and related materials. Among them, the most relevant ones with regard to their influence on the electrical conductivity of ACs are likely to be quaternary nitrogen, pyridine, and pyrrole-type structures.[154] Theoretical calculations have evidenced that nitrogen incorporation into quaternary positions creates new donor electronic states near the Fermi level, thus conferring enhanced n-type conductivity to the resulting nitrogen-doped carbon material.[154,159] This conclusion has been additionally corroborated by several experimental works focused on investigating the role of different nitrogen-containing functionalities on the electrochemical performance of biomass-derived ACs.[160,161] By contrast, pyridinic nitrogen located close to a carbon vacancy provides an additional acceptor state owing to the absence of a p_z orbital in the position of the vacancy, which leads to the

appearance of p-type conductivity.[154] As far as pyrrolic nitrogen is concerned, theoretical studies have demonstrated that this species is able to improve the electron mobility of the carbon matrix due to its electron-donor properties.[162,163] Furthermore, nitrogen atoms in a six member ring in the edge of graphene layers can be also considered as pyrrole functionalities because of the conjugation of their lone-pair electrons with the extended π system of the graphene layer. Likewise, Hulicova-Jurcakova et al. have also suggested that imides and lactams can be regarded as pyrrole-type structures,[161,164] thereby exerting similar effects on electrical conductivity of carbon materials.

Concerning the third question, a careful and comprehensive review of the available literature on the topic has revealed that nitrogen incorporation does not always lead to an improvement of electrical conductivity for the resulting carbon materials as compared to their undoped counterparts, as for example in.[165–169] Notwithstanding, it should be highlighted that such an increase in conductivity with nitrogen doping is by far the most commonly reported trend for a variety of carbon-based materials, including ACs.[126,159,170–173] In this connection, it is worth mentioning that most published works reporting experimental electrical conductivity data measured for nitrogen-doped ACs are essentially devoted to evaluate their suitability and performance as electrode materials in electrochemical energy conversion and storage devices, such as fuel cells and supercapacitors.[163,174,175] Consequently, there is an urgent need for systematic research works aimed at studying in detail and unveiling the influence of nitrogen incorporation on the electrical conductivity of ACs and related materials. Such studies should be focused not only on understanding the overall variation of this property with nitrogen concentration in the carbon matrix, but also on clarifying the specific effect of each particular nitrogen-containing functionality.

3.2.3. Influence of phosphorus-containing surface functional groups and structures

The influence of phosphorus surface functional groups and structures on the electrical properties of AC-based materials was carefully analyzed by Ramos et al. in several works.[176–178] These authors prepared a wide series of ACCs from two types of fabrics by chemical activation with different activating agents containing phosphorus under varying experimental conditions, and the effects of the process variables on the electrical properties of the resulting ACCs on a macroscopic scale were examined.

In the first work, several ACCs were developed from denim fabric by activation with phosphoric acid under inert atmosphere, the influence of both the acid concentration (from 5 to 15 wt.%) and heat treatment temperature (from 600 to 950 °C) on the electrical resistivity being systematically analyzed. Regardless of the preparation conditions, all the ACCs were electrically conductive (i.e., they obeyed to the Ohm's law), although the sample obtained by treatment at 600 °C exhibited noticeably higher resistivities as compared to the rest of carbon materials. The resistivity was found to decrease linearly with the temperature measured at the center of the surface of the ACCs, which is the typical behavior for semiconductor materials. In fact, the experimental data were fitted by the following expression:

$$\frac{\rho}{\rho_0} = 1 + \alpha_0(T - T_0) \qquad (8)$$

where ρ is the electrical resistivity at the temperature T of the ACC surface, while ρ_0 and α_0 stand for the electrical resistivity and the thermal coefficient, respectively, at the reference temperature T_0 (i.e., 0 °C). Furthermore, the samples were heated by Joule effect, leading to surface temperatures comprised in the range between 25 and 225 °C. In this regard, it is worth noting that the heat generated by the aforesaid physical effect might be enough for in situ electrothermal regeneration of ACCs loaded with VOCs, thus allowing their recovery by direct application of electrical current.[179,180] On the other hand, the authors could draw the following major conclusions by comparing the electrical resistivity values measured for ACCs prepared under different operational conditions. First, the influence of the heat treatment temperature was markedly stronger than that of the phosphoric acid concentration. Thus, for a fixed temperature the increase in the acid concentration only altered slightly the resistivity of the resulting ACCs, whereas this property significantly decreased when rising the heating temperature for a given acid concentration, probably as a consequence of the predominant development of graphitic nanodomains over that of porosity. Second, the increase in the activation degree by prolonging the time of thermal treatment at the maximum temperature resulted in an increment of resistivity, which was attributed to a greater extent of porosity development as evidenced from textural parameters.

In the second work, the effect of the inherent nature of the precursor on the electrical properties of ACCs was examined. For such an aim, ACCs were prepared from five different cellulose-based fabrics by

chemical activation with phosphoric acid under the following pre-established conditions. The starting materials were soaked in phosphoric acid solutions of 10 wt.% concentration at 100 °C for 30 min and, after oven-drying, the impregnated samples were thermally treated at 800 °C for 1 h in inert atmosphere and then rinsed with distilled hot water until neutral pH. The electrical behavior observed for all these ACCs was well in agreement with that described for their counterparts prepared in the earlier work. Thus, the samples were electrically conductive and showed the trend characteristic of semiconductor materials. The obtained results suggested that the electrical properties of the ACCs were strongly affected not only by the inherent nature of the precursor fabric, but also by their physico-chemical features, including porosity development and elemental carbon content. By taking into account these two parameters, the authors found the following empirical equation correlating them with the electrical resistivity:

$$\rho_0 = -0.80\%C + 238.0V_t - 21.2 \tag{9}$$

V_t being the total pore volume, as directly estimated from the nitrogen adsorption isotherm, and %C the elemental carbon content for the ACCs.

As a complement to the above works, these authors also employed different phosphorus-containing chemical reagents, including phosphoric acid, sodium dihydrogen phosphate, potassium dihydrogen phosphate, disodium hydrogen phosphate, and trisodium phosphate, to prepare ACCs by chemical activation of a lyocell-based precursor, in the form of woven cloth, in an attempt to shed light on their influence on the electrical properties of the resulting carbon materials.[178] The ACCs were prepared under pre-established conditions, consisting of soaking of the raw precursor with aqueous solutions of 5 wt.% concentration of each activating reagent at 60 °C overnight, followed by oven-drying, heat treatment at 864 °C for 1 h under nitrogen atmosphere, and subsequent washing with hot distilled water until neutral pH was attained. Similarly to previous results, all the ACCs developed in this work were electrically conductive and the variation of their resistivity with temperature also fitted to Equation (8), thus confirming their semiconductor behavior. Moreover, the electrical properties of these ACCs were found to depend on their physico-chemical features in a very complex way. Thus, factors such as porosity development, including specific surface area, pore size distribution, and micropore volume, and aromatization degree related to C/H atomic ratio were pointed out to likely have a significant

contribution to the overall electrical resistivity values measured for the ACCs. In an attempt to integrate the influence of all these factors for the various phosphorus compounds used as activating agents, the authors proposed the following empirical equation for the electrical resistivity:

$$\rho_0 = 12.3 + 74.8W_0 - 0.21\frac{C}{H} \tag{10}$$

where W_0 is the micropore volume and C/H the ratio of elemental carbon to hydrogen contents for the ACCs. A good agreement between experimental resistivity values and those estimated by applying the latter expression was found.

3.3. Influence of carbonization temperature and graphitization degree

In addition to the factors previously dealt with in the present review, it is also well-known that the magnitude of the electrical conductivity of AC materials strongly depends on their graphitization degree.[181] This latter feature is largely determined by both the precursor material and the conditions used in the preparation process, especially during the carbonization step. In this regard, it should be pointed out that carbonization is a common process in the production of AC by means of the two traditional activation methods, physical activation and chemical activation. Besides the employed activating agents (i.e., oxidizing gases or chemical agents), the major difference between these two methods lies on whether the carbonization and activation stages occur separately or not. Thus, while physical activation is a two-step process consisting of the carbonization of the raw material followed by the activation of the resulting pyrolytic char in the presence of suitable oxidizing gases, typically carbon dioxide, air or steam, the chemical activation involves the co-carbonization of the parent feedstock with a variety of chemical agents, such as phosphoric acid, potassium hydroxide or zinc chloride.[3,182] Therefore, irrespective of the activation method, it becomes evident that the analysis and understanding of the variation of conductivity during the carbonization stage, as a result of both compositional and microstructural changes, is crucial in order to obtain AC materials with desired electrical properties by controlling the preparation conditions and selecting the appropriate ones.

In brief, carbonization is a process consisting of a thermal decomposition, commonly named as pyrolysis, of the raw material, whereby moisture and most of the volatile matter, usually containing heteroatoms
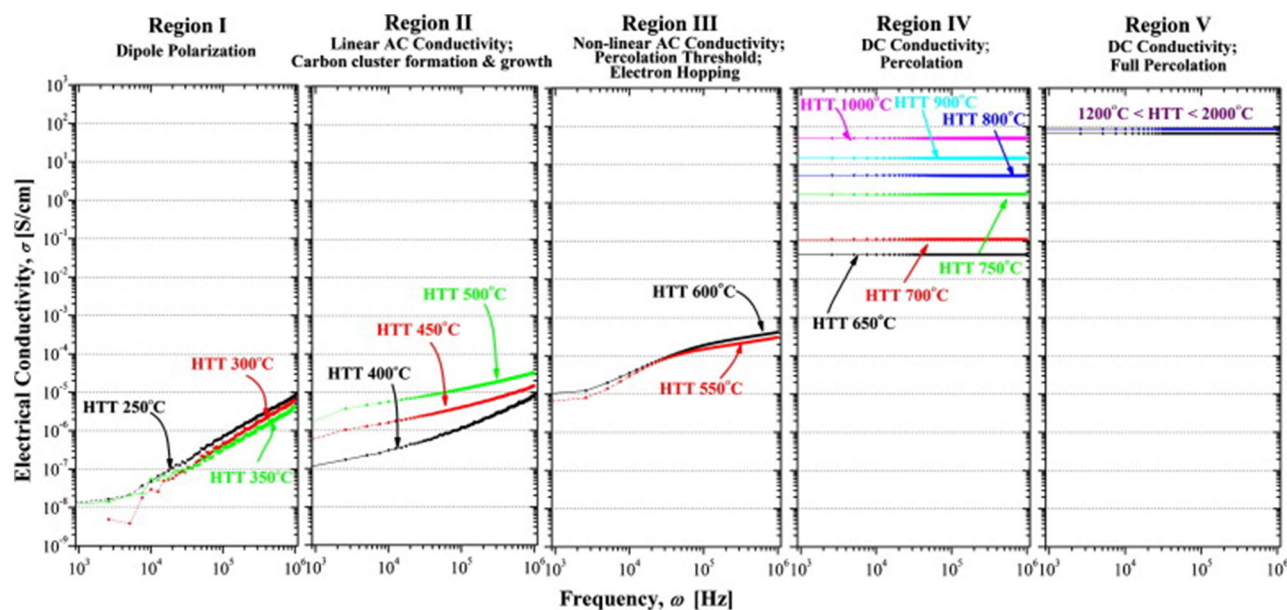
Figure 9. Regions of conductivity and microstructural evolution identified during the carbonization of microcrystalline cellulose at heat treatment temperatures (HTTs) ranging from 250 to 2000 °C. Reprinted from Rhim et al.,[186] with permission from Elsevier.

such as oxygen, nitrogen, and hydrogen, is removed. As temperature rises, a number of complex radical condensation reactions are initiated and lead to the formation of some localized graphitic units, which start to grow and become aligned into very small graphitic microcrystallites. These are stacks of several aromatic layers, usually referred to as graphene sheets.[183] The size of the graphene sheets (L_a), the stacking number (L_c), and the relative orientation of the crystallites are parameters playing a key role as they determine to a large extent the electrical conductivity of the resulting carbonized product.[16,184]

A variety of carbon precursors, such as petroleum pitch, coal pitch, and some polymers, pass through a fluid stage during the carbonization process. This fluid state, called as mesophase, allows large aromatic molecules to align each other, yielding a relatively extensive pre-graphitic structure. Because of these chars can be converted into highly ordered graphite by an additional heat treatment at temperatures above 2,500 °C, they are usually referred to as graphitizing carbons.[183] On the contrary, other precursors preserve their solid state during the whole carbonization treatment. This fact significantly hinders the mobility of the graphitic crystallites, thus resulting in the formation of a product consisting of a rigid amorphous structure formed by randomly oriented graphene layers.[185] In stark contrast to the aforementioned graphitizing carbons, these materials cannot be easily transformed into graphite by further heat treatment at high temperature, so they are called non-graphitizing carbons. Raw materials such as biomass, non-fusing coals, and some

thermosetting polymers are among the most common precursors used in the preparation of non-graphitizing carbons by carbonization.[16]

As a representative example, Rhim et al. reported the variation of the electrical conductivity and microstructure of microcrystalline cellulose as a function of the heat treatment temperature during its carbonization in the range from 250 to 2,000 °C.[186] They chose this organic compound extracted from refined wood pulp as a model material for their research because it is a basic component of wood (together with hemicellulose and lignin at varying proportions), which is one of the most employed biomass precursors for the industrial manufacture of ACs. Moreover, the use of high purity microcrystalline cellulose for this kind of studies allowed drawing confident conclusions about the carbonization mechanisms of organic compounds as they are converted to non-graphitizing carbons. As shown in Figure 9, the authors identified five distinct regions of conductivity that are directly correlated with both the chemical decomposition and microstructural evolution of the pristine cellulose during the pyrolytic treatment. At early stages of the carbonization, between 250 and 350 °C, the ac conductivity was found to increase with frequency of the applied electric field and to decrease with increasing carbonization temperature. Such behavior was ascribed to the removal of polar oxygen-containing functional groups, mainly hydroxyl, carbonyl, and ether, from the starting cellulose precursor as gaseous molecules. At this point, it is worth noting that this behavior was well in agreement with the results previously reported

by Sugimoto and Norimoto for blocks of several woods (sugi, hinoki, and lauan) subjected to heat treatment at increasing temperatures between 200 and 800 °C under inert atmosphere.[187,188] After this first region, ac conductivity started to increase with heat treatment temperature up to 500 °C as a result of the formation and growth of highly conductive carbon nanoclusters. A further increase in conductivity was observed between 550 and 600 °C as these nanoclusters grew in size so they were close enough to each other to allow electron hopping and tunneling between them.[189,190] Furthermore, over this temperature range the ac conductivity exhibited a non-linear frequency dependency due to electron hopping, interfacial polarization, and onset of a percolation threshold. Once more, these observations were in line with the results observed by Sugimoto and Norimoto for sugi wood specimens carbonized at similar temperatures.[187] In the region comprised between 610 and 1,000 °C, conductivity was independent of frequency (i.e., DC conductivity) and it kept rising with heat treatment temperature owing to the growth and further percolation of the aforesaid carbon clusters. Regarding this, it should be noted that the abrupt transition from frequency dependent to frequency independent ac conductivity observed between 600 and 610 °C suggested that the percolation threshold was reached between these two very close carbonization temperatures. Finally, the carbonized material reached a fully percolated state in the range from 1,200 to 2,000 °C, so that the dc conductivity remained nearly constant with increasing heat treatment temperature.

Another example was provided by Barroso-Bogeat et al., who investigated the influence of the carbonization temperature on the dc electrical conductivity of chars derived from vine shoots, a common agricultural waste generated in most of the European Mediterranean countries after the grape harvest.[5] They found that the conductivity of the carbonized samples increased by three orders of magnitude as the carbonization temperature rose from 600 to 900 °C. These results appeared to be well in agreement with those previously reported for a variety of biomass precursors subjected to carbonization treatments at similar temperatures, such as rice husk[80] and straw,[191] oil palm fiber,[192] Babassu nut,[83] corncob,[193] bamboo,[194] lignin,[195–198] several woods,[82,187,189,199–203] and so forth. The authors explained the observed variation of electrical conductivity with increasing heat treatment temperature on the basis of the chemical decomposition, degree of conversion to carbon, and microstructural evolution of the vine shoots components during the carbonization process. According to a previous work published by the same authors,[11] the pyrolysis of vine shoots was almost complete at 600 °C. The resulting carbonized product was mainly composed of carbon atoms arranged in turbostratic microcrystallites,[203–206] which in turn were embedded in an amorphous carbon matrix with very low conductivity, typically reported for other carbonized organic materials.[186,203] Such microcrystallites were very small in size and located too far away to allow effective conduction by electron hopping and tunneling between them, thus resulting in a very poor electrical conductivity for the sample carbonized at 600 °C. The additional slight loss of mass when rising the pyrolysis temperature up to 900 °C was ascribed to a small removal of heteroatoms, chiefly hydrogen, leading to an increase in the carbon to hydrogen atomic ratio, and thereby in the aromatization degree, for the resulting carbon product. An explanation based on band theory for this steady increase in electrical conductivity with increasing aromatization degree was first provided by Mrozowski and collaborators in the early 1950's.[204,207] As hydrogen atoms are progressively released from the edge of graphene layers, some of the σ-electrons belonging to carbon atoms which were bounded to hydrogen are left unpaired. Some of these atoms become bonded to neighboring aromatic rings, thus enlarging the size of the graphene layers. However, for those carbon atoms remaining unpaired, a π-electron is able to jump from the π-band into the σ-state, forming a spin pair and creating a hole at the top of the π-band. Consequently, a great number of holes (i.e., positive charge carriers) are generated and such a phenomenon may account for the enhancement in conductivity with increasing carbonization temperature. At this point, it is worth noting that a similar correlation between the carbon to hydrogen atomic ratio (i.e., the aromatization degree) and the electrical resistivity had been also observed earlier by Kumar and Gupta for Acacia and Eucalyptus wood chars prepared by carbonization at several temperatures ranging from 400 to 1,200 °C.[199] Moreover, for carbonized woods the electrical conductivity has been reported to strongly change depending on the carbonization temperature. Thus, at pyrolysis temperatures below 500 °C the resulting wood chars behave as insulator materials, while carbonization at or above 800 °C entails a drastic increase in conductivity.[208] Finally, when heat-treated at 1,800 °C the carbonized product becomes a good electrical conductor.[181]
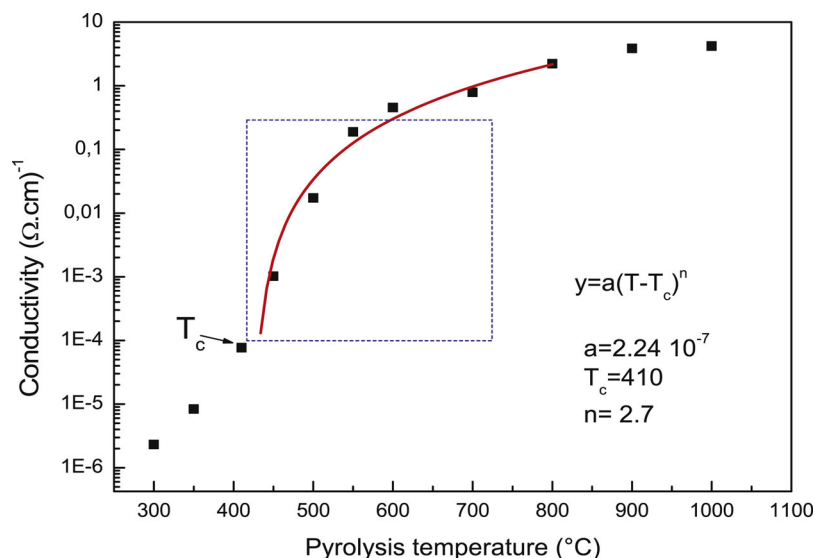
Figure 10. Variation of the DC electrical conductivity as a function of the carbonization temperature for a series of AC pellets prepared from olive stones by chemical activation with phosphoric acid. Reprinted from Djeridi et al.,[209] with permission from Elsevier.

On the other hand, Djeridi et al. studied the effect of pyrolysis temperature on the dc electrical conductivity for a series of AC pellets.[209] These were prepared from olive stones, a biomass precursor widely employed in the manufacture of ACs, by chemical activation with phosphoric acid at $110\,°C$ for $9\,h$ followed by a carbonization step under nitrogen atmosphere for $3\,h$ at different temperatures comprised between 350 and $1,000\,°C$. They found that conductivity steeply increased for those carbon samples obtained at carbonization temperatures in the range from 410 to $600\,°C$. This behavior was unambiguously connected with the partial conversion of amorphous carbon into graphitic nanodomains, as evidenced from the emergence of reflection peaks ascribable to graphite in the X-ray diffraction patterns corresponding to the AC samples pyrolyzed above $500\,°C$, and also with the presence of a percolation threshold. According to the percolation theory, above this threshold conducting paths are formed in the carbon matrix, thus resulting in a conversion from an insulator to a conductor material. Therefore, a critical conduction temperature (T_c) was defined as the pyrolysis temperature corresponding to the onset of the formation of conducting paths. As illustrated in Figure 10, such a temperature was estimated by fitting the conductivity versus pyrolysis temperature plot to the following power law:[210]

$$\sigma = A \cdot (T - T_c)^n \qquad (11)$$

where σ is the dc electrical conductivity of the AC sample, T stands for the carbonization or pyrolysis temperature, while A and n are both fitting constants. They obtained the best fit for a T_c value of $410\,°C$.

More recently, Hoffmann et al. assessed the electrical conductivity of three corncob-derived chars prepared by carbonization under nitrogen atmosphere following two different heating programs.[76] In the first one, the raw material was heated at either 600 or $800\,°C$ for $1\,h$, while the second program consisted of heating the corncob first at $300\,°C$ for $1\,h$ and then at $900\,°C$ also for $1\,h$. As expected, the carbon content in the resulting chars notably increased with the pyrolysis temperature from 600 to $900\,°C$, whereas the opposite applies to the oxygen content. Such trends were connected with the progressive reorganization of the carbon atoms in the sample into randomly oriented polyaromatic carbon sheets (i.e., graphitic domains) as the carbonization temperature is increased.[211] These graphitic domains are well-known to be conducting, so that the electrical conductivity of the as-prepared chars also increased with the pyrolysis temperature. According to the available literature, the authors attempted to explain these results on the basis of a set of underlying processes: (i) an increase in the ash content of the chars with increasing carbonization temperature,[212] (ii) the gradual transformation from sp^3-hybridised carbon atoms involved in σ-type bonds, which were predominant in the corncob precursor, to conjugated sp^2-hybridised carbon atoms as the carbonization progresses, thus resulting in an electronic delocalization intimately related with the electrical conduction,[213] (iii) the removal of acidic oxygen-containing functional groups and structures

on the carbon surface, which behave as a barrier for electrons hindering their flow, at pyrolysis temperatures above 600–700 °C,[213,214] and (iv) the aforementioned reorganization of the carbon atoms from an amorphous state to graphitic crystalline structures, ultimately leading to graphite at high enough heat treatment temperatures (i.e., above 2,500 °C).[16] Among them, the contribution of the increasing ash content was found to be almost negligible as compared to the other processes occurring during carbonization,[76] especially the progressive structural reorganization leading to an increase in the graphitization degree.

Particular attention should be also paid to non-conventional carbonization methods, such as catalytic and hydrothermal carbonization, and their influence on the graphitization degree and hence on the electrical conductivity of the resulting char products.

As far as catalytic carbonization methods are concerned, several works have tested a variety of metal-based catalysts, including aluminum isopropoxide,[181] iron (III) oxide[191,195] and nitrate,[191] and nickel (II) acetate,[198] to obtain wood- and lignin-derived chars, and further analyze the evolution of their conductivity with the carbonization temperature. In this regard, it is worth highlighting that with the presence of the aforementioned metal catalysts the onset of the graphitization usually occurs at notably lower carbonization temperatures in comparison to conventional heat treatment methods.

Nishimiya et al. prepared several char samples from Japanese cedar wood in a series of successive steps consisting of conventional carbonization under nitrogen atmosphere at 500 °C, followed by impregnation with an aluminum isopropoxide solution in isopropanol for 24 h, and a final heat treatment by the direct electric pulse heating method.[181] When measuring the electrical conductivity of the resulting carbonized samples and compared to a char prepared by the conventional carbonization method, the authors found that the addition of aluminum improved the conductivity, but no clear correlation between the conductivity and the aluminum content was observed. Based on X-ray diffraction and X-ray photoelectron spectroscopy analyses, this effect was ascribed to larger graphitization degrees reached at lower temperatures due to the catalytic role played by aluminum, the formation of any carbon-aluminum bond being completely ruled out.

Xiao et al. applied two different carbonization methods in order to prepare lignin-derived chars with low electrical resistivity for electromagnetic shielding purposes.[195] In the first one, mixtures of lignin and the iron (III) oxide catalyst with several mass ratios (i.e., 50:1, 20:1, and 2:1 lignin:catalyst) were carbonized in nitrogen atmosphere at 900 °C for 30 min, whereas for the second method the raw lignin was first pre-carbonized at 400 °C for 30 min, then mixed with the catalyst at the same mass ratios, and finally carbonized at either 900 or 1,400 °C for 30 min. For the sake of comparison, they also prepared some additional char samples by conventional carbonization at temperatures ranging from 600 to 1,400 °C. The electrical resistivities of the carbon products resulting from the first catalytic method were clearly higher than those measured for the conventional chars, a fact tentatively attributed to the contamination of the iron (III) oxide catalyst by volatile compounds evolved during the lignin pyrolytic process.[215] On the contrary, lignin pre-carbonization followed by catalytic carbonization avoided catalyst deactivation and yielded chars exhibiting resistivity values quite similar and even lower than those for their counterparts obtained by non-catalysed carbonization. Again, these latter results were connected with a certain development and growth of graphitic domains, which were too small in size to be unambiguously identified by the X-ray diffraction technique. In a previously published work, the same authors had also compared the catalytic performance of iron (III) oxide and nitrate for the carbonization of rice straw at 900 °C for 30 min under nitrogen atmosphere and using different straw to catalyst mass ratios.[191] Iron (III) nitrate was reported to be successful as a carbonization catalyst in the preparation of low resistivity chars, while no beneficial effect was noticed when iron (III) oxide was tested.

In recent years, methods of hydrothermal carbonization have received a great deal of attention as promising alternatives to conventional pyrolysis in the preparation of carbonized precursors for ACs.[216] Among a number of advantages, hydrothermal carbonization allows a great homogenization of the biomass precursors, removes mineral matter, avoids drying, provides a high carbon yield, and shows a good heat balance owing to its exothermic nature.[217] Within this context, the influence of the hydrothermal carbonization conditions on the electrical conductivity of the resulting ACs emerges as an issue of major concern, which has been first investigated in a systematic way by Lee et al.[218] They prepared four carbonized precursors by hydrothermal carbonization of glucose at two different temperatures (i.e., 180 and 240 °C), and for two different times (i.e., 12 and 24 h).

The resulting carbonized samples were subsequently subjected to chemical activation with potassium hydroxide. Strikingly, the textural features of the as-prepared ACs were almost unaffected by both the temperature and time of the hydrothermal carbonization, so that the carbon samples displayed quite similar textural parameters. On the contrary, their electrical conductivities were markedly different. Specifically, a higher conductivity was obtained for the ACs prepared from precursors hydrothermally carbonized at higher temperature and shorter reaction time. Similar results were also reported for AC samples prepared from sugarcane bagasse by hydrothermal carbonization at 200, 250, and 300 °C for 6 h and further chemical activation with potassium hydroxide aqueous solution for 24 h.[219] Therefore, it becomes apparent the need for optimizing the hydrothermal carbonization conditions in order to prepare ACs featuring the desired conductivity values with a view to specific applications, like electrode materials in supercapacitors.

4. Effect of adsorption of gases and vapors on the electrical conductivity of activated carbons and related materials

The change in the electrical conductivity of carbon conductors when exposed to an atmosphere of a certain gas or vapor has been known for a long time.[220–224] This phenomenon was first tentatively attributed to variations in the contact resistances between the granules or particles of the carbon material.[222,223] By assuming this explanation, the swelling of carbon particles on adsorption of the gaseous adsorbate should increase the contact area and the number of conduction paths between them, thus resulting in a decreased resistance regardless of the nature of the vapor. Likewise, the shrinkage of carbon particles on desorption would cause a resistance increase. Nevertheless, for carbon materials showing very large surface area to volume ratios, such as ACs, it was expected that surface effects coming from their interaction with the adsorbate may have a great influence on the conductivity of the material. Within this context, the pioneering works concerning the influence of the physical adsorption of gases and vapors on the electrical conductivity of AC were conducted by McIntosh et al.[120,225] in the late 1940's and early 1950's.

In a first publication, the authors reported the variations in the electrical resistance and length of AC rods prepared by chemical activation with zinc chloride as a result of the physical adsorption of a variety of vapors, including saturated and unsaturated hydrocarbons with chain lengths up to four carbon atoms, water, carbon dioxide, ethylene oxide, dimethyl ether, sulfur dioxide, ethyl chloride, and ammonia. Both the extent and direction of the resistance changes at a fixed temperature were found to depend on the chemical nature of the molecules of the gaseous adsorbate, this phenomenon being by far more complicated than had been previously presumed. On the basis of the dimensional and resistance variations for the rods and the absence of any correlation between them, it was concluded that the mechanical alteration of the contact resistances between the carbon aggregates did not suffice to explain the experimental results. Such conclusion was evidenced by comparing the effects caused by the adsorption of butane and ethyl chloride. Both adsorbates brought about a noticeable increase in the length of the rod, which was greatest near saturation of the AC surface. However, the variation of resistance in this region was almost negligible for butane, whereas a marked change was noticed in the case of ethyl chloride. Accordingly, it was postulated that the adsorbates may modify either the mobility or the number of conduction electrons in the carbon adsorbent.

The results provided in the above work were further completed by determining the adsorption isotherms and the associated electrical resistance changes at several temperatures for six saturated hydrocarbons containing from one to four carbon atoms, as well as for ethyl chloride, on the same type of AC rods as those investigated in the previous paper. It was observed that the adsorption of all hydrocarbons led to a decrease in resistance, being this greater with increasing amount of adsorbed vapor, until the resistance values appeared to reach a limit asymptotically. In fact, the variation of the electrical resistance as a function of the amount adsorbed could be expressed by the following empirical equation:

$$\frac{V}{\left(\frac{1}{R} - \frac{1}{R_0}\right)} = C + D\left(\frac{1}{R} - \frac{1}{R_0}\right) \qquad (12)$$

where V designates the adsorbed volume of hydrocarbon, R denotes the measured resistance of the AC rod, R_0 is the resistance of the outgassed rod, and C and D are constants at a given temperature. Such expression was shown to be valid in the range up to two thirds of the maximum adsorbed volume. In addition, the magnitude of the resistance change at a certain temperature and adsorbed volume was also found to be proportional to the number of carbon atoms of

the adsorbate molecule. This finding seemed to confirm that the physically adsorbed saturated hydrocarbon molecules tend to lie with their major axis on the surface of the carbon adsorbent, as had been previously suggested by measurements of heats of adsorption.[226,227] On the other hand, the resistance of the AC rods was notably increased by chemisorption of oxygen in order to elucidate the influence of the number of electrons in the conduction band of the carbon solid on the effect of the different hydrocarbon adsorbates. Strikingly, both the variation of the electrical conductivity by the physically adsorbed vapors and the adsorption isotherms were not modified by small amounts of chemisorbed oxygen. Nevertheless, changes of the original resistance values of the AC rods by the successive treatments with oxygen were noted. Such an effect was attributed to an increased localization of conduction electrons as a consequence of the chemisorption of oxygen on surface carbon atoms with unsaturated valence bonds, which are considered to act as electron donors. In stark contrast, the behavior observed for ethyl chloride was significantly more complicated in comparison to that for the saturated hydrocarbons. For such an adsorbate, the direction and magnitude of the resistance alteration were dependent both on the volume of adsorbed vapor and the temperature.

In brief, the above works allow concluding that the experimental data may be only accounted for on the postulate that the presence of physically adsorbed molecules on the carbon surface alters the number of conduction electrons rather than their mobility.

After a long parenthesis of nearly six decades, interest in the issue of the influence of physical adsorption of hydrocarbons on the electrical properties of ACs and related materials appears to have reemerged in recent years. This renewed attention is chiefly based on a dual purpose: the feasibility of in situ electrothermal regeneration of ACCs after the adsorption of VOCs on the one hand,[228] and the use of AC-based materials as gas sensors on the other.[229–231]

Ramos et al. prepared a couple of ACC samples from a lyocell-based fabric precursor by impregnation with 10 wt.% phosphoric acid solution at 60 °C overnight and subsequent heat treatment at a maximum temperature of 864 or 963 °C for 1 h under nitrogen atmosphere.[228] The electrical resistance of both ACCs before and after adsorption of n-hexane was measured in order to assess the viability of regenerating these carbon adsorbents loaded with VOCs by Joule effect. For such an aim, the prepared ACCs were exposed in an environment saturated with n-hexane for 48 h as a

way to ensure that their saturation capacity had been reached. Similarly to the results previously reported by the same authors for a series of ACCs prepared by chemical activation with phosphoric acid under varying conditions,[176–178] these cloth samples obtained at two different heat treatment temperatures were also electrically conductive and showed a semiconductor behavior before and after the physical adsorption of n-hexane. Furthermore, the resistivity of the ACC samples prior to n-hexane exposure was found to increase with heat treatment temperature, likely as a result of the higher porosity development reflected in the values of specific surface area, total pore volume, and micropore volume estimated from the adsorption isotherms of nitrogen, carbon dioxide, and several organic compounds. As expected, the adsorption of n-hexane reduced the resistivity of both ACCs, the decrease being greater for the sample prepared at 963 °C due to the higher amount of hydrocarbon adsorbed on it. A similar trend had been also observed earlier for a lab-made AC monolith at different uniform loadings of toluene both from experimental data and theoretical calculations using a mathematical model.[232] In this case, the resistivity decreased linearly as the adsorbate loading increased, according to the empirical relationship $\rho = 0.77 - 0.168q$, where q stands for the amount of toluene adsorbed by mass unit of adsorbent. The following explanation based on the electronic band structure of semiconductors was proposed for this phenomenon (the application of this model to ACs and related materials will be dealt with in greater detail in a later section of the present review). Electrical conduction in these materials is connected with the creation of holes in the valence band as a consequence of the thermal promotion of electrons to the conduction band. Physically adsorbed molecules are supposed to interact with these thermally excited electrons, so that their mobility is reduced. This fact would largely avoid electron-hole recombination processes and increase the number of holes, thus enhancing the conductivity of the carbon material.

The electrical resistivity as well as its change due to physical adsorption of isobutane were analyzed for activated carbon fiber cloths (ACFCs, hereafter) with nano-tailored physical and chemical properties, and the obtained results were attempted to explain on the basis of the modifications affecting the nanographitic structure of these carbon materials.[229] A series of three commercial novoloid-based ACFCs having nominal surface areas of around 1,000, 1,500, and 2,000 m^2·g^{-1} were chemically modified by treatment
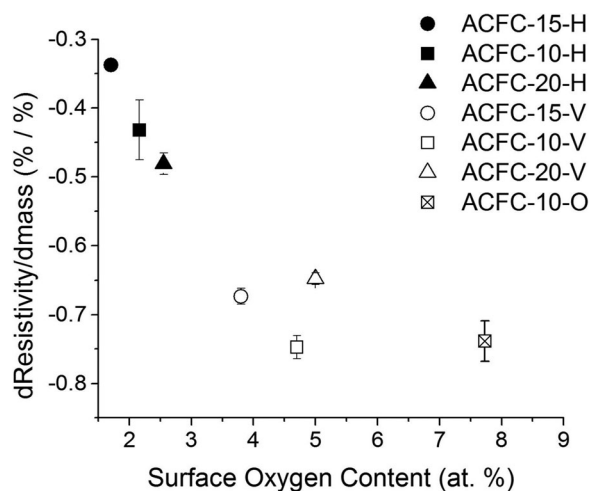
Figure 11. Percentage change in resistivity for a series of ACFC samples after a complete adsorption cycle of 1% iso-butane in nitrogen normalized by percentage change in ACFC mass (dResistivity/dmass) as a function of the sample surface oxygen content. The two digits of the samples' identification refer to the nominal surface area values (10: 1000 $m^2 \cdot g^{-1}$, 15: 1500 $m^2 \cdot g^{-1}$, and 20: 2000 $m^2 \cdot g^{-1}$), while the final letter denotes the sample treatment (V: untreated sample, H: hydrogen treatment at 900 °C for more than 8 h, O: nitric acid treatment at 24 °C for more than 8 h). Reprinted from Johnsen et al.,[229] with permission from Elsevier.

with hydrogen at 900 °C and with nitric acid at 24 °C for more than 8 h. After these reducing and oxidizing treatments, samples with micropore volumes ranging from 0.35 to 0.92 $cm^3 \cdot g^{-1}$ and surface oxygen contents between 1.7 and 7.7 at.% were obtained. Concerning the influence of the physical adsorption of isobutane, both the initial resistivity value and its decrease after a complete adsorption cycle of 1% isobutane in nitrogen increased with the micropore volume and surface oxygen content of the ACFCs. The larger decrease in resistivity after an adsorption cycle with increasing micropore volume was directly connected with the higher adsorption capacity, since the adsorbed iso-butane enlarges the interlayer spacing between the nanographene sheets from 0.382 to 0.415 nm, resulting in a reduction of the distance between nanographitic domains and thereby in an increased electron hopping. However, the effect of surface oxygen content was by far more complex, affecting the change in resistivity per unit mass of isobutane adsorbed rather than the adsorption capacity. As depicted in Figure 11, increasing oxygen for ACFC samples having low surface oxygen contents (i.e., below 3.8 at.%) increased the percentage change in resistivity due to isobutane adsorption, while for those with higher surface oxygen contents (i.e., from 3.8 to 7.7 at.%) the effect on this value was negligible. Therefore, the obtained results allowed concluding that the ability of ACFCs to detect

the adsorbed mass of isobutane based on resistivity changes can be improved by increasing their surface oxygen content up to a threshold value comprised in the range between 2.6 and 3.8 at.%.

Besides the aforementioned hydrocarbon adsor-bates, the effect of the adsorption of other gases, such as nitrogen, oxygen, nitric oxide, nitrous oxide, sulfur dioxide, and water, both on the structural and elec-trical properties of activated carbon fibers (referred to as ACFs henceforward) has also been explored by sev-eral authors.[233,234] First, Imai and Kaneko investigated the change in the electrical conductivity at 30 °C upon adsorption of several gases for a single pitch-based ACF, which had been previously characterized in terms of its textural features.[233] As shown in Figure 12, they observed two opposite trends depend-ing on the electron affinity of the adsorbate molecule. On the one hand, conductivity increased upon expos-ing to oxygen and sulfur dioxide, thus revealing that holes are the dominant charge carriers. Because of their great electron affinity, both molecules are able to accept electrons from surface carbon atoms with the concomitant creation of an identical number of holes. On the other hand, adsorption of nitric oxide, nitrous oxide, and water led to a decrease of conductivity. Based on these findings, the authors proposed a linear relationship between the logarithm of the maximum electrical conductivity change due to gas chemisorp-tion and the electron affinity of the adsorbate mol-ecule, which is depicted in Figure 12. Such a relationship appears to indicate that the conductivity change is attributed to charge transfer adsorption of adsorbate molecules on the surface of micrographitic crystallites. In a subsequent work, Kobayashi et al. employed a commercial phenol-based ACF showing a specific surface area of around 2,000 $m^2 \cdot g^{-1}$, which was subjected to measurements of electron spin reson-ance (ESR) spectroscopy, magnetic susceptibility, and electrical conductivity before and after gas adsorp-tion.[234] The conductivity of the ACF sample, recorded 20 min after the introduction of the gas at room tem-perature, decreased with oxygen or nitrogen pressure at values below 0.1 kPa. Next, it tended to saturate and eventually reached a nearly constant value at pressures above 0.5 kPa, irrespective of the gaseous adsorbate. Although the conductivity behavior after the adsorption of oxygen and nitrogen was essentially the same, the extent of the reduction was slightly lower for the former (i.e., 13% for oxygen as com-pared to 15% for nitrogen). In line with previous works, these experimental results were explained on the basis of the structural modification induced by gas adsorption. If an electron transport mechanism
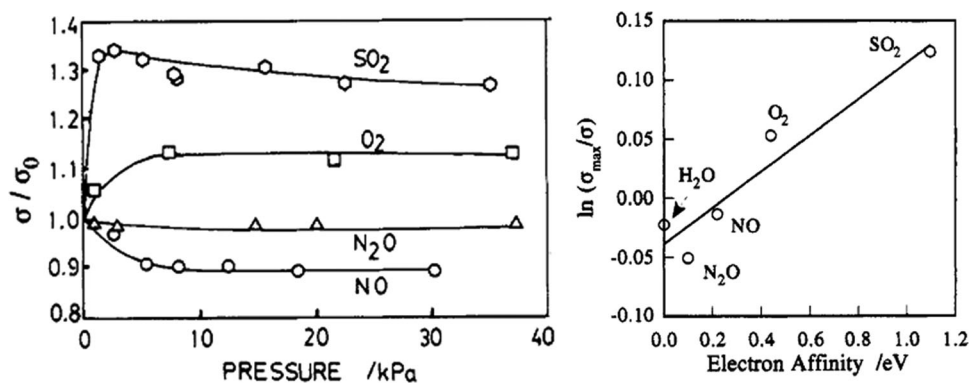
Figure 12. Variation in electrical conductivity upon adsorption of several gases (left) and relationship between electrical conductivity change and the electron affinity of adsorbate molecule (right) for a single pitch-derived ACF. Reprinted with permission from Imai and Kaneko.[233] Copyright © 1992 American Chemical Society.

governed by hopping between highly conductive nanographitic domains is assumed for ACFs,[235,236] then the swelling of these nanodomains as a consequence of the adsorption of gaseous species will result in an increase in the distance between them and thereby in a conductivity decrement. The time dependence of conductivity under the presence of oxygen or nitrogen gas was also investigated over a wide temporal range. After the introduction of oxygen, the conductivity suddenly dropped for about 30 s, the decrease being greater with increasing oxygen pressure (i.e., 5% for 0.12 kPa and 9% for 0.59 kPa). Then, the conductivity steadily increased with a long time tail extending over 50 h. This behavior was firstly associated with the change in the amount of adsorbed oxygen with time. In this regard, a slow chemisorption process has been reported to occur during oxygen adsorption on AC, whose rate is markedly slower in comparison with that of physisorption.[237] Furthermore, the slow chemisorption gives rise to an increase of hole carriers by means of charge transfer from nanographitic domains to adsorbed oxygen molecules.[204,238] By contrast, the above time evolution of conductivity was not observed under nitrogen atmosphere, except for the initial steep decrease after the introduction of the gaseous adsorbate.

On the other hand, the effect of ammonia adsorption on the electrical properties of a commercial wood-based AC (BAX-1500, Mead-Westvaco), as received and after a strong oxidizing treatment with 50% nitric acid for 5 h, has been recently analyzed with a view to its potential application as sensing material in gas sensor devices.[230] Upon exposure to 100 ppm ammonia and subsequent purging with air, the resistance changes registered for the pristine and oxidized carbon samples followed opposite trends. Thus, the original AC showed a 27% gradual increase in resistance for 1 h before reaching stabilization,

while after oxidation the resulting carbon sample exhibited a 60% decrease in resistance, requiring less than 30 min to attain equilibrium. This markedly different behavior suggests that the aforesaid oxidation treatment altered the electrical properties of the raw AC. As far as the initial carbon sample is concerned, holes are the predominant charge carriers, so that adsorption of ammonia, which is a well-known electron donating molecule, causes their depletion and thereby a resistance increase. On the contrary, the surface of the oxidized sample possesses a great number of oxygen and nitrogen-containing functional groups and structures, most of which are considered as electron donating and hence contribute to the hole annihilation of the carbon material and its conversion to a n-type semiconductor. Consequently, subsequent exposure to ammonia gas results in a decrease of resistance as compared to the unoxidized AC sample.

Finally, in a recently published work Kempiński demonstrated that an effect of resistivity switching can be achieved for ACFs by a combination of adsorption of specific molecules and application of an external electric field.[239] Starting from a set of commercial phenol resin-derived ACFs with low oxygen contents and amounts of defects in graphene layers, as well as with relatively high graphitization degrees and varying porosities, their electrical resistivities were registered at different temperatures (typically 29 and 67 K) after adsorption of helium and water. Resistivity jumps were noticed for the first time in ACF samples when turning on the external 3 kV·cm^{-1} electric field. These observed jumps were found to be dependent both on the temperature and the adsorbed molecule (see Figure 13). Thus, for the ACF with a nominal surface area of 2,000 m^2·g^{-1} the absolute amplitude of the jump decreased by a factor of around 5.7 with temperature increase from 29 to 67 K, whereas the
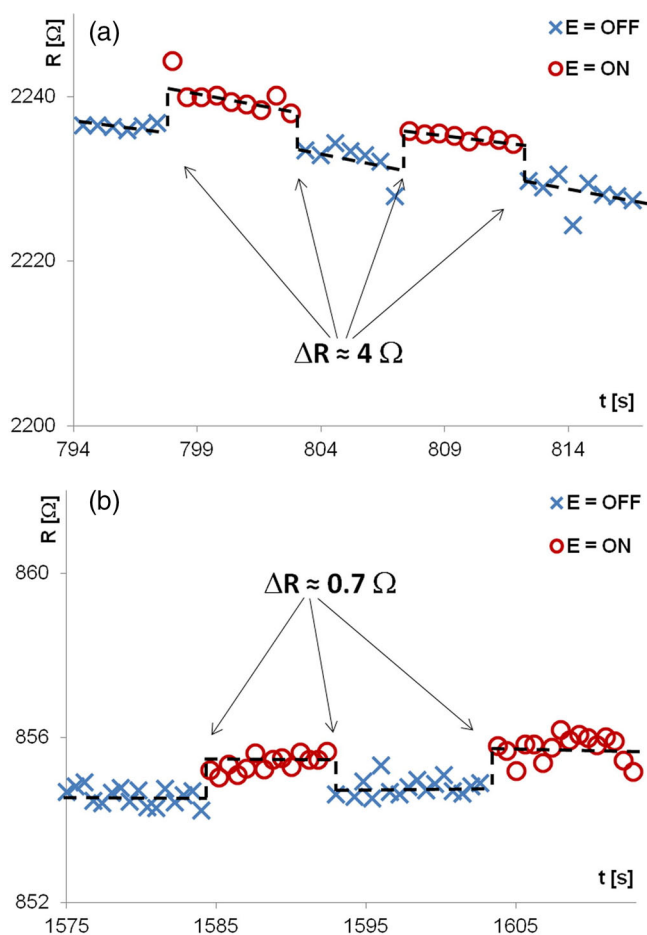
Figure 13. Switching effect in a water-filled ACF at different temperatures: (a) 29 K and (b) 67 K. Turning on the electric field ($E = 3\,kV\cdot cm^{-1}$) caused a resistance jump (ΔR), which depended on the temperature. Dashed lines only serve as an eye guide, whereas arrows indicate the switching events. Reprinted from Kempiński,[239] with permission from Elsevier.

switching effect was only observed after adsorption of water. This latter observation allowed postulating that such effect could be caused by the spatial ordering of adsorbed dipolar molecules along the external field direction, which increased the local potential barriers for hopping of charge carriers within the fibers. At this point, it should be highlighted that the results and conclusions derived from this research could be quite interesting with a view to developing carbon-based sensors of gas and liquid substances with enhanced selectivity and sensitivity.

5. Temperature dependence of electrical conductivity in activated carbons and related materials

Electrical conductivity measurements, and especially its temperature dependence, have been traditionally regarded as a powerful tool to gain insight into the electronic band structure and electric conduction process in semiconductors, such as ACs and related materials.[240] Therefore, it is extremely interesting to include in the present review a section aimed at briefly reviewing the most relevant works concerning the temperature dependence of conductivity in ACs, as well as the different proposed mechanisms for electrical conduction on the basis of experimental data.

The temperature dependence of the electrical conductivity for AC materials was first investigated by McIntosh et al.[120,225] These authors found that the variation of the resistance of several AC rods with temperature obeyed the following linear relationship:

$$\log R = A - B \cdot T \qquad (13)$$

where R denotes the electrical resistance, T the temperature, and both A and B are constants. According to the above equation, the electrical resistance decreases with increasing temperature, which is the typical behavior of semiconductor materials. Although a similar behavior had been previously reported by Mrozowski[204,241] for a variety of carbon materials, obtained by heat treatment of organic precursors under inert atmosphere at increasing temperatures and ranging from the so-called raw cokes to polycrystalline graphite through baked carbons, these works constitute the first experimental evidence of semiconductivity in ACs.

On the basis of the similarities both in the preparation conditions and resistance values for the baked carbons studied by Mrozowski and the aforementioned AC rods, it was assumed that the high electrical conductivity of the latter arises almost entirely from the presence of a large and essentially constant number of free electrons in the conduction band, in addition to the very low number of them activated from the valence band, over the whole investigated temperature range. These excess electrons are considered to be associated with peripheral carbon atoms at the surface discontinuities of the solid and also with those around lattice imperfections, which have unsaturated valence bonds. They drop down from their energy states into the bottom of the conduction band, thus becoming free and mobile electrons and contributing to conductivity.[204,241] Within this theoretical framework, the resistance dependence on temperature observed for AC rods (Equation (13)) could be primarily explained by a decreased scattering of electrons in the polycrystalline graphitic structure of the carbon material with increasing temperature.[120]

The temperature dependence of the electrical conductivity has been also studied for highly oxidized AC materials. In particular, Barton and Koresh measured

the resistance as a function of temperature for a commercial carbon cloth oxidized by air at 400 °C, by refluxing with nitric acid, and by a combination of both treatments, and subsequently subjected to heat treatment at different temperatures up to 900 °C under inert atmosphere.[121] In the same line, similar experiments were performed by Polovina et al. over samples prepared by different oxidative treatments of a lab-made ACC with air, nitric acid, hydrogen peroxide, and iron (III) nitrate, and then also heat-treated at temperatures below 900 °C in argon atmosphere.[123] The obtained results were well in agreement regardless of the origin of the carbon cloth, the oxidizing agent, and the oxidation treatment conditions. The resistance was found to decrease with increasing temperature, thus confirming the typical semiconductor behavior for all the oxidized ACC samples. Such a behavior was tentatively attributed to an abrupt insulator-to-metal transition, in a similar way to that previously reported for a series of heat-treated amorphous carbons.[242] As already discussed in the present review, the temperature-dependent electrical conductivity for semiconductors follows a mechanism of thermal activation, so that the experimental data should be fitted by this Arrhenius-type equation:

$$\ln \sigma = \ln \sigma_0 - \frac{E_g}{2k_B T} \quad (14)$$

or expressed in terms of electrical resistance:[123]

$$\ln R = \ln R_0 + \frac{E_g}{2k_B T} \quad (15)$$

Nonetheless, the resulting plots were only linear at lower temperatures, suggesting that the activation energy for electron conduction was not constant over the entire investigated temperature range. Therefore, the activation energy was estimated for each ACC sample from the slope of the low temperature linear section of the corresponding Arrhenius plot. According to Fritzsche,[243] the activation energy value in amorphous semiconductors, as these ACCs can be considered, is directly related with the energy gap or band gap (E_g) of the material.

As summarized in Table 1, the band gap markedly increased for the oxidized samples as compared to their raw carbon cloths, whereas the opposite applied to a given oxidized or non-oxidized sample when the heat treatment temperature increased. Moreover, these effects were as a rule more pronounced with increasing oxidizing power of the chemical agent and heating temperature. Both trends are unambiguously connected with the formation and thermal decomposition of a variety of oxygen-containing groups and

structures on the carbon cloth surface as a result of the different oxidizing and heat treatments, respectively. At that time, the authors were only able to provide a qualitative theoretical explanation for the influence of surface oxides on the electronic properties of the ACCs. It was based on the simplest assumption that the major energy barrier to electron conduction is located at the graphitic crystallite boundaries. The oxidation of these boundaries is expected to bring about an enlargement of the band gap and thereby a significant reduction in the number of available electrons in the conduction band of the carbon material. Furthermore, they also speculated that such an increase in the band gap should be lower for oxygen complexes anchored to highly graphitic domains than for those situated on less organized carbon structures.

By analyzing the variation of electrical resistivity with temperature on the basis of a thermally activated process (i.e., by using Equation (15)), similar correlations between the band gap energy and the oxygen content (see Table 2) have been also noted for commercial ACFC samples, with different activation levels and chemically modified by treatment with a mixture of concentrated nitric and sulfuric acids for 5 days, and with pure hydrogen at 950 °C for 3 h. In addition, the resistivity dependence on temperature for this series of ACFC samples was also fitted to the following equation:

$$\rho = \rho_0 + \rho_0 \alpha_0 (T - T_0) \quad (16)$$

where ρ is the electrical resistivity at the temperature T of the ACFC, whilst ρ_0 and α_0 denote the electrical resistivity and the thermal coefficient, respectively, at the reference temperature T_0, usually taken at 0 °C (i.e., 273.15 K). At this point, it should be highlighted that although the above expression is typically used to describe the variation of resistivity with temperature in metallic materials, it has also been extensively applied in literature to a number of carbon-based materials within a limited temperature range.[124,125,244–247] Both for virgin and chemically-treated ACFCs, the resistivity decreased with increasing temperature in the interval from 20 to 225 °C, thus confirming their expected semiconductor behavior and leading to negative values of the thermal coefficient. In this regard, the latter varied between $-3.7 \cdot 10^{-3}$ and $-1.1 \cdot 10^{-3}$ K^{-1} for these carbon samples, being well in agreement with those values previously estimated for rayon-based ACFC,[125] pitch-based ACF,[248] AC monolith, and AC beads.[247] Moreover, it was found that the sensitivity (i.e., the absolute value of α_0) of ACFC to temperature variation notably increased with the specific surface area.

Table 1. Energy gap values (E_g) estimated for carbon cloths oxidized by several oxidizing agents and subsequently heat-treated at different temperatures (*HTT*) under inert atmosphere. Adapted from Barton and Koresh[121] and Polovina et al.,[123] with permission from Elsevier.

Carbon sample	Oxidizing treatment	HTT, °C	E_g, eV
Commercial carbon cloth	Air at 400 °C	400	0.058
	1. Air at 400 °C for 40 h 2. Refluxing with 6 mol·L⁻¹ aqueous nitric acid for 1 h	900	0.037
	Refluxing with 6 mol·L⁻¹ aqueous nitric acid for 16 h	250	0.071
		400	0.036
		900	0.016
Lab-made activated carbon cloth	–	338	0.076
		866	0.049
	Concentrated nitric acid at 90 °C for 1 h	427	0.095
		606	0.100
		865	0.054
	Iron (III) nitrate at 140 °C for 1 h	331	0.141
		866	0.054

5.1. Temperature dependence of electrical conductivity in ACFs

In addition to their inherent commercial interest, ACFs are considered as an excellent material to investigate strong localization and disorder related phenomena in the electron transport properties, mainly owing to their unusually high density of defects.[249] Nevertheless, similarly to ACs, the electrical properties of ACFs have been scarcely studied.[250] The more relevant findings concerning the temperature dependence of electrical conductivity in ACFs are discussed below, with special attention to the involved conduction mechanisms.

Firstly, it is worth noting that the fiber geometry provides greater measurement sensitivity in order to investigate several transport properties of these carbon materials.[249] Furthermore, the interest in ACFs with regard to the study of electron transport is also connected with the fact that this material represents a natural three-dimensional granular metallic system rather than other consisting of thin films.[251]

Di Vittorio et al. reported a preliminary survey of the temperature dependence of the dc electrical conductivity for pitch-based ACFs with specific surface area of around $1,000 \, \text{m}^2 \cdot \text{g}^{-1}$.[235,236] As the most relevant points, they measured a low conductivity value ($\sim 600 \, \text{S·m}^{-1}$) at room temperature in comparison with that registered for single crystal graphite ($\sim 2.5 \cdot 10^6 \, \text{S·m}^{-1}$) and,[252] similarly to other carbon materials, a great decrease in conductivity was observed at low temperatures, being indicative of semiconductor behavior. The experimental temperature-dependent conductivity data for these ACFs were successfully fitted to the 2D variable range hopping (VRH) mechanism, mathematically expressed by the following equation:

$$\sigma = \sigma_0 \cdot \exp\left[-\left(\frac{T}{T_0} \right)^{-\frac{1}{3}} \right] \quad (17)$$

A subsequent work focused on measuring the temperature dependence of electrical conductivity for a series of ACF samples prepared from different precursors and having specific surface areas ranging from 1,000 to $2,000 \, \text{m}^2 \cdot \text{g}^{-1}$ showed that their conductivity-temperature plots are rather similarly shaped, irrespective of both the specific surface area value and precursor[253] (see Figure 14). Nevertheless, the conductivity at a given temperature was found to rise with specific surface area as well as with the disorder degree of the precursor material. In this connection, the greater the disorder, the larger the number of hopping sites and the lower the distance between them, thus leading to an increase of the likelihood of hopping and thereby of electrical conductivity.

Dresselhaus et al. studied the influence of the heat treatment temperature on the electronic transport properties of ACFs.[252] As shown in Figure 15, the conductivity appeared to be essentially independent of temperature for carbon samples heat-treated at 1,500 °C and above. This is the typical behavior observed for weakly disordered fibers with domain of band conduction, being boundary scattering the dominant scattering mechanism. Such dramatic changes in transport properties of ACFs as a consequence of thermal treatment have been associated with the occurrence of an insulator-metal transition. Unlike the trend reported for the above ACFs, conductivity decreases with increasing surface area and disorder degree for those fibers subjected to heat treatment at temperatures higher than 1,500 °C.[253] In order to get insight into the aforementioned insulator-metal transition, the same authors accomplished a series of electron transport measurements on phenol and pitch-

Table 2. Energy gap values (E_g) estimated for virgin and chemically modified commercial activated carbon fiber cloths. Adapted from Hashisho et al.,[124] with permission from Elsevier.

Carbon sample	Oxidizing/reducing treatment	E_g, eV
Commercial ACFC ($S_{BET} = 849$ m^2·g^{-1})	–	0.061
	1/1 (v/v) mixture of concentrated nitric and sulfuric acids for 120 h	0.122
	Pure hydrogen at 950 °C for 3 h	0.031
Commercial ACFC ($S_{BET} = 1335$ m^2·g^{-1})	–	0.083
	1/1 (v/v) mixture of concentrated nitric and sulfuric acids for 120 h	0.126
	Pure hydrogen at 950 °C for 3 h	0.056
Commercial ACFC ($S_{BET} = 1566$ m^2·g^{-1})	–	0.076
	1/1 (v/v) mixture of concentrated nitric and sulfuric acids for 120 h	0.036
	Pure hydrogen at 950 °C for 3 h	0.060
Commercial ACFC ($S_{BET} = 1763$ m^2·g^{-1})	–	0.071
	1/1 (v/v) mixture of concentrated nitric and sulfuric acids for 120 h	0.042
	Pure hydrogen at 950 °C for 3 h	0.048

derived ACFs heat-treated under inert atmosphere at several temperatures ranging from 300 to 2,500 °C.[251,253,254] Obtained results clearly confirmed an insulator-metal transition for those samples heated between 1,000 and 1,200 °C.[251,253] Moreover, it is worth noting that the conductivity value at which the transition occurred was well in agreement with that of Mott's minimum metallic conductivity.[251]

Kuriyama and Dresselhaus carried out a more thorough study on the dc electrical conductivity over a wide temperature range between 30 and 300 K for phenolic ACFs with nominal values of specific surface area from 1,000 to 2,000 m^2·g^{-1}.[45] A positive temperature dependence of conductivity was found, in line with the semiconductor behavior typically observed for other disordered carbon materials. Furthermore, this temperature dependence was nearly linear for the entire investigated temperature range. These authors also fitted the temperature-dependent electrical conductivity data to a model involving two intrinsic conduction mechanisms, VRH process between localized states and thermal activation process. The former is dominant at very low temperatures (i.e., below 40 K) and appears to be temperature-independent above 30 K. Conversely, the latter mechanism obeys to a classical Arrhenius-type law and dominates at higher temperatures since the charge carriers acquire enough energy to overcome the potential barrier. Both the term associated with the VRH mechanism and the pre-exponential factor of the thermal activated process increase with the specific surface area of the ACFs, while the opposite applies to the activation energy. Similar results were subsequently reported by Nakayama et al.[248]

Conduction by carrier hopping can only be sensitively studied at very low temperatures, near absolute zero. For this reason, Fung et al. measured the electrical conductivity of ACFs prepared from two different precursors (isotropic pitch and phenol) down to 4 K.[249] They fitted the experimental temperature-dependent conductivity to the Mott's law, obtaining the best fits with an exponent of $n = 1/2$, and interpreted this behavior on the basis of three feasible mechanisms: 1D VRH, Coulomb gap conduction (CGC), and charge-energy-limited tunneling conduction (CELTC), which exclusively differ in the expression for the parameter T_0 in Equation (17). Among them, CELTC was the only model providing meaningful values for its physical parameters, so that this conduction mechanism is likely to be the dominant at low temperature. Such mechanism is commonly observed in granular metallic systems, to which ACFs closely resemble, where a certain charging energy is required for the generation of charge carriers and the conduction of these carriers takes place by tunneling between conductive grains.[251,255,256] Nonetheless, the application of the CELTC model to porous carbon materials, such as ACFs, has been criticized chiefly because of its limitations and unrealistic assumptions. Aimed at overcoming these drawbacks, Fung et al. proposed a new conduction model based on VRH mechanism near a Coulomb gap around the Fermi level due to carrier-carrier interactions.[257] Such a Coulomb gap variable range hopping (CGVRH) conduction model has also been successfully applied to explain the temperature dependence of electrical conductivity in ACFs prepared from pitch and phenol and heat-treated at temperatures ranging from 300 to 2,500 °C[251] and, more recently, in commercial phenol resin-derived ACFs.[239,258]

6. Electronic band structure models for activated carbons and related materials

Over the last seventy years, several attempts have been conducted and reported in order to describe the electronic properties of carbonaceous materials, including ACs, by means of the band model of electronic
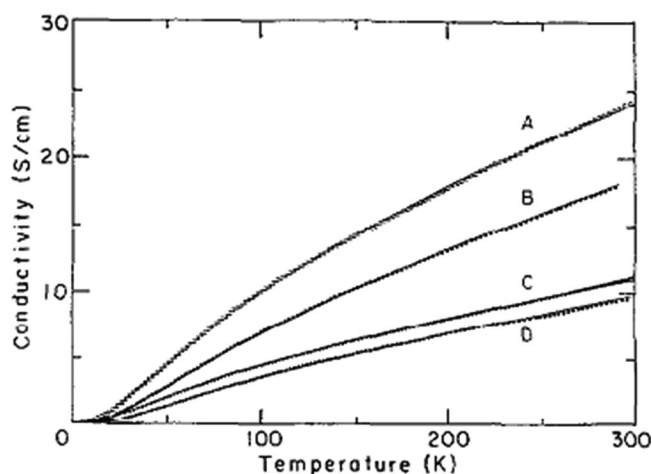
Figure 14. Temperature dependence of electrical conductivity for a series of phenol-based ACFs featuring different specific surface area values. A: long fibers, 2000 m²·g⁻¹, B: short fibers, 2000 m²·g⁻¹, C: short fibers, 1200 m²·g⁻¹, and D: long fibers, 1000 m²·g⁻¹. Reprinted from Dresselhaus et al.,[236] with permission from Elsevier.

Figure 15. Temperature dependence of the electrical conductivity, plotted as lnσ vs T, for a phenol-based ACF submitted to heat treatment at several temperatures. Reprinted from Dresselhaus et al.,[236] with permission from Elsevier.

energies,[207,259,260] typically applied to metal, semiconductor, and insulator materials. Nonetheless, the major and common problem regarding these works arises from the fact that AC is neither a metal nor a semiconductor and, although often referred to as "amorphous," it exhibits a special short range order closely resembling graphite crystallites on a nanometer scale.[261] Very complex electronic band structures, derived from quantum mechanics, have been proposed and discussed for amorphous semiconductors.[259] As a distinctive feature, the movement of charge carriers (i.e., electrons) in these structures is considered to take place by hopping between energy states more or less localized along the band gap,[260,262,263] in a rather similar way to that reported for conducting polymers.[264] Obviously, all these models make use of concepts related to solid-state physics. In this context, Kastening proposed a different and novel approach to this problem by an alternative model for electronic properties, including electrical conductivity, of ACs using concepts more amenable and familiar to solid state chemists.[261] Accordingly, because of its relative simplicity in comparison to other models based on high level physics, the next paragraph will be focused on highlighting the key points of the Kastening's model.

The aforesaid model is based on the assumption of a nanostructure for AC consisting of graphite nanocrystals, so-called domains henceforth, which form the walls of the pores and usually contain about three graphene layers with lengths ranging from 2 to 4 nm perpendicular to the c-axis and separated by a distance of
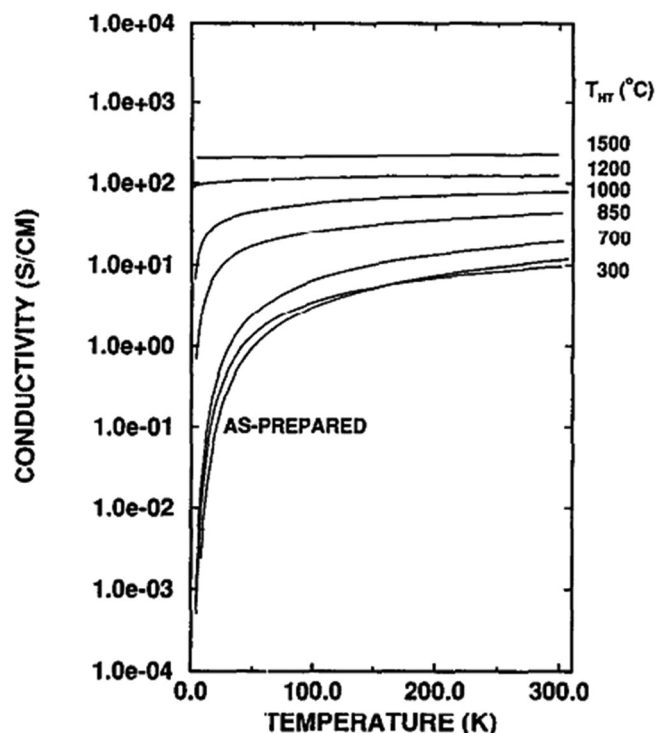
0.373 nm,[261,265] as well as on a set of experimental data concerning the variation of the conductivity, the thermoelectric power, and the electron spin resonance (ESR) signal of AC, immersed in electrolyte solutions, on changing the electrode potential.[264] According to this nanostructure, the author distinguished between three types of charge carriers (i.e., electrons or holes): (i) delocalized throughout the whole particle of carbon material, (ii) delocalized throughout a single domain, and (iii) localized at a single atom or atomic group. Among them, both types (i) and (ii) are expected to contribute to the electrical conductivity of AC. However, the electronic states belonging to type (i) appear to be completely unoccupied, so their contribution to the overall measured conductivity should be almost negligible. The theoretical model establishes that the graphene domains are charged either with one, and preferentially two, electrons or uncharged, with the coherent π-electron system being delocalized throughout the entire single domain. All these different types of domains are in thermodynamic equilibrium with each others. Under this scenario, the charge transport is regarded as transport of charged domains, thus resembling the conduction involving protons in solvents with an extensive network of hydrogen bonds such as water and termed Grotthus mechanism,[266] whereas uncharged domains do not contribute to the

electrical conductivity. As its major advantage, it should be highlighted that this theoretical model allows an easy and direct correlation with complex electronic energy band models by constructing electronic levels from the energetic data.

7. Summary and outlook

From the comprehensive literature review conducted in the present paper, it becomes apparent that research activity concerning the electrical properties of ACs and related materials will keep on growing in the near future. Such a prediction is based on the steadily increasing use of these carbon materials as electrode components in electrochemical energy conversion and storage devices, like supercapacitors, lithium-ion batteries, and fuel cells. In this regard, it is well-established that the electrical properties, particularly conductivity, play a pivotal role on the application and performance of ACs in the aforementioned systems. Furthermore, several novel applications of ACs, chiefly in the fields of electroadsorption, electrocatalysis, sensors, and actuators, are also intimately related with their excellent and unique electrical properties. Accordingly, the accurate measurement of these properties, as well as their understanding and rationalization, are essential with a view to assessing many of the current and future technological applications of ACs.

The accurate measurement of electrical conductivity for granular and powdered ACs is a quite difficult task, and it usually requires the application of low to moderate compression in order to ensure the electrical contact between neighboring carbon particles and grains. Once a proper contact has been achieved, the conductivity is usually measured by the two-probe method or the four-probe method, this latter being frequently preferred to the former. Estimated conductivity values are the result of a complex interplay between a number of factors, among which the intrinsic conductivity of the single particles or grains (i.e., the so-called intraparticle conductivity), the degree of contact between them, and their packing should be highlighted.

Intrinsic conductivity is mainly determined by the texture, surface chemistry, and degree of graphitization of AC, which are well-known to strongly depend on the nature of the feedstock and the preparation method, including both the activating agent and the operational conditions. Careful selection and control of the carbon precursor and the preparation conditions (carbonization temperature, time and

atmosphere, activation method, activating agent, activation temperature and time, and so forth) are essential to tailor the graphitization degree, textural features, and surface chemistry of the resulting ACs, thus allowing optimizing their electrical conductivity for the requirements of specific technical applications. Moreover, intrinsic conductivity of ACs and related materials is also influenced in a significant manner by the adsorption of chemical species, in particular oxygen, water, and hydrocarbons.

On the other hand, analysis of the temperature dependence of electrical conductivity is considered as a powerful tool to gain insight into the electronic band structure and electron conduction process in ACs. Similar to graphite and other carbon-based materials, ACs are generally agreed to behave as semiconductor materials, which entails that their electrical conductivity increases with temperature. Several mechanisms have been proposed to describe the electron conduction in ACs depending on the temperature range, encompassing from an easy thermally activated process obeying to the Arrhenius equation to more complex mathematical models, such as the variable range hopping. Nevertheless, none of these models is able to satisfactorily describe the electron conduction mechanism in AC-based materials over the entire temperature range. Therefore, further investigations are required in this direction to solve such an open question.

ORCID

Adrián Barroso Bogeat ⓘ http://orcid.org/0000-0002-1272-3834

References

1. R. C. Bansal, J. B. Donnet, and F. Stoeckli, *Active Carbon*, Marcel Dekker, New York (1988).
2. F. Rodríguez-Reinoso, Production and applications of activated carbons. In *Handbook of Porous Solids*, F. Schüth, K. S. W. Sing, and J. Weitkamp (eds.), Wiley, Weinheim, 1766–1827 (2002).
3. H. Marsh and F. Rodríguez-Reinoso, *Activated Carbon*, Elsevier, Amsterdam (2006).
4. M. Olivares-Marín, J. A. Fernández, M. J. Lázaro, C. Fernández-González, A. Macías-García, V. Gómez-Serrano, F. Stoeckli, and T. A. Centeno, Cherry

stones as precursor of activated carbons for supercapacitors, *Mater. Chem. Phys.* **114**(1), 323–327 (2009).

5. A. Barroso-Bogeat, M. Alexandre-Franco, C. Fernández-González, A. Macías-García, and V. Gómez-Serrano, Temperature dependence of the electrical conductivity of activated carbons prepared from vine shoots by physical and chemical activation methods, *Microporous Mesoporous Mater.* **209**, 90–98 (2015).

6. H. Jankowska, A. Świątkowski, and J. Choma, *Active Carbon*, Ellis Horwood, Chichester (1991).

7. T. J. Bandosz, ed., *Activated Carbon Surfaces in Environmental Remediation*, 1st ed., Elsevier, Amsterdam (2006).

8. J. M. Dias, M. C. M. Alvim-Ferraz, M. F. Almeida, J. Rivera-Utrilla, and M. Sánchez-Polo, Waste materials for activated carbon preparation and its use in aqueous-phase treatment: A review, *J. Environ. Manage.* **85**(4), 833–846 (2007).

9. M. A. Yahya, Z. Al-Qodah, and C. Ngah, Agricultural bio-waste materials as potential sustainable precursors used for activated carbon production: A review, *Renew. Sustain. Energy Rev.* **46**, 218–235 (2015).

10. P. González-García, Activated carbon from lignocellulosics precursors: A review of the synthesis methods, characterization techniques and applications, *Renew. Sustain. Energy Rev.* **82**, 1393–1414 (2018).

11. M. Ruiz-Fernández, M. Alexandre-Franco, C. Fernández-González, and V. Gómez-Serrano, Development of activated carbon from vine shoots by physical and chemical activation methods. Some insight into activation mechanisms, *Adsorption.* **17**(3), 621–629 (2011).

12. P. Serp and J. L. Figueiredo, *Carbon Materials for Catalysis*, John Wiley & Sons, Hoboken (2009).

13. E. Frackowiak and F. Béguin, Carbon materials for the electrochemical storage of energy in capacitors, *Carbon N. Y.* **39**(6), 937–950 (2001).

14. J. Gamby, P. L. Taberna, P. Simon, J. F. Fauvarque, and M. Chesneau, Studies and characterisations of various activated carbons used for carbon/carbon supercapacitors, *J. Power Sources.* **101**(1), 109–116 (2001).

15. A. González, E. Goikolea, J. A. Barrena, and R. Mysyk, Review on supercapacitors: Technologies and materials, *Renew. Sustain. Energy Rev.* **58**, 1189–1206 (2016).

16. A. G. Pandolfo and A. F. Hollenkamp, Carbon properties and their role in supercapacitors, *J. Power Sources.* **157**(1), 11–27 (2006).

17. A. Burke, R&D considerations for the performance and application of electrochemical capacitors, *Electrochim. Acta.* **53**, 1083–1091 (2007).

18. F. Béguin, E. Raymundo-Piñero, and E. Frackowiak, Electrical double-layer capacitors and pseudocapacitors. In *Carbons for Electrochemical Energy Storage and Conversion Systems*, F. Béguin and E. Frąckowiak (eds.), CRC Press, Boca Raton, 329–375 (2010).

19. A. Davies and A. Yu, Material advancements in supercapacitors: From activated carbon to carbon nanotube and graphene, *Can. J. Chem. Eng.* **89**(6), 1342–1357 (2011).

20. Y. Zhai, Y. Dou, D. Zhao, P. F. Fulvio, R. T. Mayes, and S. Dai, Carbon materials for chemical capacitive energy storage, *Adv. Mater.* **23**(42), 4828–4850 (2011).

21. A. Ghosh and Y. H. Lee, Carbon-based electrochemical capacitors, *ChemSusChem.* **5**(3), 480–499 (2012).

22. L. Wei and G. Yushin, Nanostructured activated carbons from natural precursors for electrical double layer capacitors, *Nano Energy.* **1**(4), 552–565 (2012).

23. J. Wang and S. Kaskel, KOH activation of carbon-based materials for energy storage, *J. Mater. Chem.* **22**(45), 23710–23725 (2012).

24. Y. P. Wu, E. Rahm, and R. Holze, Carbon anode materials for lithium ion batteries, *J. Power Sources.* **114**(2), 228–236 (2003).

25. J. C. Arrebola, A. Caballero, L. Hernán, J. Morales, M. Olivares-Marín, and V. Gómez-Serrano, Improving the performance of biomass-derived carbons in Li-ion batteries by controlling the lithium insertion process, *J. Electrochem. Soc.* **157**(7), A791–A797 (2010).

26. P. Novák, D. Goers, and M. E. Spahr, Carbon materials in lithium-ion batteries. In *Carbons for Electrochemical Energy Storage and Conversion Systems*, F. Béguin and E. Frąckowiak (eds.), CRC Press, Boca Raton, 263–328 (2010).

27. R. J. Brodd, Carbon in batteries and energy conversion devices. In F. Béguin and E. Frąckowiak (eds.), *Carbons for Electrochemical Energy Storage and Conversion Systems*, CRC Press, Boca Raton, 411–428 (2010).

28. P. Kalyani and A. Anitha, Biomass carbon & its prospects in electrochemical energy systems, *Int. J. Hydrogen Energy.* **38**, 4034–4045 (2013).

29. X. Peng, J. Fu, C. Zhang, J. Tao, L. Sun, and P. K. Chu, Rice husk-derived activated carbon for Li Ion battery anode, *Nanosci. Nanotechnol. Lett.* **6**(1), 68–71 (2014).

30. S. Sankar, S. Saravanan, A. T. A. Ahmed, A. I. Inamdar, H. Im, S. Lee, and D. Y. Kim, Spherical activated-carbon nanoparticles derived from biomass green tea wastes for anode material of lithium-ion battery, *Mater. Lett.* **240**, 189–192 (2019).

31. C. Li, J. Li, Y. Zhang, X. Cui, H. Lei, and G. Li, Heteroatom-doped hierarchically porous carbons derived from cucumber stem as high-performance anodes for sodium-ion batteries, *J. Mater. Sci.* **54**(7), 5641–5657 (2019).

32. C. Lamy, Fuel cell systems: Which technological breakthrough for industrial development? In *Carbons for Electrochemical Energy Storage and Conversion Systems*, F. Béguin and E. Frąckowiak (eds.), CRC Press, Boca Raton, 377–410 (2010).

33. D. Cao, G. Wang, C. Wang, J. Wang, and T. Lu, Enhancement of electrooxidation activity of activated carbon for direct carbon fuel cell, *Int. J. Hydrogen Energy.* **35**(4), 1778–1782 (2010).

34. J. Zhang, Z. Zhong, D. Shen, J. Zhao, H. Zhang, M. Yang, and W. Li, Preparation of bamboo-based

activated carbon and its application in direct carbon fuel cells, *Energy Fuels.* **25**(5), 2187–2193 (2011).

35. J. Zhang, Z. Zhong, J. Zhao, M. Yang, W. Li, and H. Zhang, Study on the preparation of activated carbon for direct carbon fuel cell with oak sawdust, *Can. J. Chem. Eng.* **90**(3), 762–768 (2012).

36. L.-D. Tsai, H.-C. Chien, C.-H. Wang, C.-M. Lai, J.-N. Lin, C.-Y. Zhu, and F.-C. Chang, Poly(ethylene glycol) modified activated carbon for high performance proton exchange membrane fuel cells, *Int. J. Hydrogen Energy.* **38**(26), 11331–11339 (2013).

37. P. Balakrishnan, I. I. G. Inal, E. Cooksey, A. Banford, Z. Aktas, and S. M. Holmes, Enhanced performance based on a hybrid cathode backing layer using a biomass derived activated carbon framework for methanol fuel cells, *Electrochim. Acta.* **251**, 51–59 (2017).

38. L. Fan, J. Wang, L. Zhao, N. Hou, T. Gan, X. Yao, P. Li, Y. Zhao, and Y. Li, Effects of surface modification on the reactivity of activated carbon in direct carbon fuel cells, *Electrochim. Acta.* **284**, 630–638 (2018).

39. L. L. Zhang, Y. Gu, and X. S. Zhao, Advanced porous carbon electrodes for electrochemical capacitors, *J. Mater. Chem. A.* **1**(33), 9395–9408 (2013).

40. M. Zhi, C. Xiang, J. Li, M. Li, and N. Wu, Nanostructured carbon-metal oxide composite electrodes for supercapacitors: A review, *Nanoscale.* **5**(1), 72–88 (2013).

41. P. J. Hall, M. Mirzaeian, S. I. Fletcher, F. B. Sillars, A. J. R. Rennie, G. O. Shitta-Bey, G. Wilson, A. Cruden, and R. Carter, Energy storage in electrochemical capacitors: Designing functional materials to improve performance, *Energy Environ. Sci.* **3**(9), 1238–1251 (2010).

42. J. Sánchez-González, F. Stoeckli, and T. A. Centeno, The role of the electric conductivity of carbons in the electrochemical capacitor performance, *J. Electroanal. Chem.* **657**(1-2), 176–180 (2011).

43. F. Maillard, P. A. Simonov, and E. R. Savinova, Carbon materials as supports for fuel cells electrocatalysts. In *Carbon Material for Catalysis*, P. Serp and J. L. Figueiredo (eds.), John Wiley & Sons, Hoboken, 429–480 (2009).

44. H. Wang, P. Cheng, and Y. Wang, Advanced electrocatalytic performance of activated carbon prepared from asphalt, *Int. J. Electrochem. Sci.* **13**, 3257–3266 (2018).

45. K. Kuriyama and M. S. Dresselhaus, Photoconductivity of activated carbon fibers, *J. Mater. Res.* **6**(5), 1040–1047 (1991).

46. F. Skaupy and O. Kantorowicz, Das verhalten pulverförmiger metalle unter druck, *Z. Elektrochem. Angew. Phys. Chem.* **37**, 482–485 (1931).

47. F. Skaupy and O. Kantorowicz, Die elektrische leitfähigkeit pulverförmiger metalle unter druck, *Met. Met. Met.* **10**, 45–47 (1931).

48. P. L. Walker and F. Rusinko, Determination of the electrical resistivity of particulate carbons, *Fuel.* **36**(1), 43–50 (1957).

49. S. Mrozowski, Studies of carbon powders under compression. In *Proceedings of the Third Conference on Carbon*, S. Mrozowski, M. L. Studebaker, and P. L. Walker (eds.), Pergamon, Buffalo, 495– 508 (1959).

50. S. Marinković, Č. Sužnjević, and M. Djordjević, Pressure dependence of the electrical resistivity of graphite powder and its mixtures, *Phys. Stat. Sol. (a).* **4**(3), 743–754 (1971).

51. K.-J. Euler, The conductivity of compressed powders. A review, *J. Power Sources.* **3**(2), 117–136 (1978).

52. A. Espinola, P. M. Miguel, M. R. Salles, and A. R. Pinto, Electrical properties of carbons-resistance of powder materials, *Carbon N. Y.* **24**(3), 337–341 (1986).

53. N. Deprez and D. S. McLachlan, The analysis of the electrical conductivity of graphite powders during compaction, *J. Phys. D: Appl. Phys.* **21**(1), 101–107 (1988).

54. A. Celzard, J. F. Marêché, F. Payot, and G. Furdin, Electrical conductivity of carbonaceous powders, *Carbon N. Y.* **40**(15), 2801–2815 (2002).

55. B. Marinho, M. Ghislandi, E. Tkalya, C. E. Koning, and G. de With, Electrical conductivity of compacts of graphene, multi-wall carbon nanotubes, carbon black, and graphite powder, *Powder Technol.* **221**, 351–358 (2012).

56. F. J. Chacón, M. L. Cayuela, A. Roig, and M. A. Sánchez-Monedero, Understanding, measuring and tuning the electrochemical properties of biochar for environmental applications, *Rev. Environ. Sci. Biotechnol.* **16**(4), 695–715 (2017).

57. G. Giraud, J. P. Clerc, and E. Guyon, Étude par des mesures de résistance electrique de la répartition des pressions dans un empilement désordonné de sphères, *Powder Technol.* **35**(1), 107–111 (1983).

58. F. I. Zorin, Electric resistivity of powdered graphites, *Inorg. Mater.* **22**, 47–49 (1986).

59. A. Gervois, M. Ammi, T. Travers, D. Bideau, J.-C. Messager, and J.-P. Troadec, Importance of disorder in the conductivity of packings under compression, *Phys. A Stat. Mech. Appl.* **157**(1), 565–569 (1989).

60. J. P. Troadec and D. Bideau, Importance du désordre dans la conductivité de matériaux granulaires sous compression, *Onde Électrique.* **71**, 30–33 (1991).

61. H. Braun and P. Herger, On the separation of the contributions of powder particle cores and intergranular contacts to the electric resistivity of compressed powder materials, *Mater. Chem.* **7**(6), 787–802 (1982).

62. J. Sánchez-González, A. Macías-García, M. F. Alexandre-Franco, and V. Gómez-Serrano, Electrical conductivity of carbon blacks under compression, *Carbon N. Y.* **43**(4), 741–747 (2005).

63. A. Barroso-Bogeat, M. Alexandre-Franco, C. Fernández-González, A. Macías-García, and V. Gómez-Serrano, Electrical conductivity of activated carbon–metal oxide nanocomposites under compression: A comparison study, *Phys. Chem. Chem. Phys.* **16**(45), 25161–25175 (2014).

64. J. D. Bernal, A geometrical approach to the structure of liquids, *Nature.* **183**(4655), 141–147 (1959).

65. R. Ben Aïm and P. Le Goff, La Coordinance des Empilements Désordonnés de Sphères. Application aux Mélanges Binaires de Sphères, *Powder Technol.* **2**, 1–12 (1968).

66. J. A. Dodds, The porosity and contact points in multicomponent random sphere packings calculated by a simple statistical geometric model, *J. Colloid Interface Sci.* **77**(2), 317–327 (1980).

67. J. P. Troadec, A. Gervois, D. Bideau, and L. Oger, Coordinance of a spherical impurity in a disordered packing of equal spheres, *J. Phys. C: Solid State Phys.* . **20**(8), 993–1004 (1987).

68. A. Bertei and C. Nicolella, A comparative study and an extended theory of percolation for random packings of rigid spheres, *Powder Technol.* **213**(1-3), 100–108 (2011).

69. A. Barroso-Bogeat, M. Alexandre-Franco, C. Fernández-González, J. Sánchez-González, and V. Gómez-Serrano, Electrical conductivity of metal (hydr)oxide–activated carbon composites under compression. A comparison study, *Mater. Chem. Phys.* **152**, 113–122 (2015).

70. R. Holm. *Electric Contacts: Theory and Applications*, 4th ed., Springer Verlag, Berlin (1967).

71. T. Travers, D. E. Bideau, A. Gervois, J. P. Troadec, and J. C. Messager, Uniaxial compression effects on 2D mixtures of "hard" and "soft" cylinders, *J. Phys. A Math. Gen.* **19**(16), L1033–L1038 (1986).

72. F. Radjai, M. Jean, J. J. Moreau, and S. Roux, Force distributions in dense two-dimensional granular systems, *Phys. Rev. Lett.* **77**(2), 274–277 (1996).

73. F. Radjai, D. E. Wolf, M. Jean, and J.-J. Moreau, Bimodal character of stress transmission in granular packings, *Phys. Rev. Lett.* **80**(1), 61–64 (1998).

74. M. Sahimi, *Applications of Percolation Theory*, Taylor & Francis, London (1994).

75. L. R. Brodd and A. Kosawa, Primary batteries. In *Techniques of electrochemistry*, E. Yeager and A. J. Salkind (eds.), Wiley-Interscience, New York, 3, 199–289 (1978).

76. V. Hoffmann, C. Rodriguez Correa, D. Sautter, E. Maringolo, and A. Kruse, Study of the electrical conductivity of biobased carbonaceous powder materials under moderate pressure for the application as electrode materials in energy storage technologies, *GCB Bioenergy.* **11**(1), 230–248 (2019).

77. Y. Singh, Electrical resistivity measurements: A review, *Int. J. Mod. Phys. Conf. Ser.* **22**, 745–756 (2013).

78. L. B. Coleman, Technique for conductivity measurements on single crystals of organic materials, *Rev. Sci. Instrum.* **46**(8), 1125–1126 (1975).

79. M. B. Heany, Electrical conductivity and resistivity. In *Electrical Measurement, Signal Processing, and Displays*, J. G. Webster (ed.), CRC Press, Boca Raton, 7–1–7-14 (2003).

80. L. J. Kennedy, J. J. Vijaya, and G. Sekaran, Electrical conductivity study of porous carbon composite derived from rice husk, *Mater. Chem. Phys.* **91**(2-3), 471–476 (2005).

81. N. Konikkara, L. J. Kennedy, U. Aruldoss, and J. J. Vijaya, Electrical conductivity studies of nanoporous carbon derived from leather waste: Effect of pressure, temperature and porosity, *J. Nanosci. Nanotechnol.* **16**(8), 8829–8838 (2016).

82. J. G. Hernandez, I. Hernandez-Calderon, C. A. Luengo, and R. Tsu, Microscopic structure and electrical properties of heat treated coals and eucalyptus charcoal, *Carbon N. Y.* **20**(3), 201–205 (1982).

83. F. G. Emmerich, J. C. de Sousa, I. L. Torriani, and C. A. Luengo, Applications of a granular model and percolation theory to the electrical resistivity of heat treated endocarp of babassu nut, *Carbon N. Y.* **25**(3), 417–424 (1987).

84. J. S. Mattson, *Activated Carbon: Surface Chemistry and Adsorption from Solution*, Marcel Dekker, New York (1971).

85. L. R. Radovic, Surface chemistry of activated carbon materials: State of the art and implications for adsorption. In *Surfaces Nanoparticles Porous Mater*, J. A. Schwarz and C. I. Contescu (eds.), Marcel Dekker, New York, 529–565 (1999).

86. H. P. Boehm, Surface oxides on carbon and their analysis: A critical assessment, *Carbon N. Y.* **40**(2), 145–149 (2002).

87. T. J. Bandosz and A. Co, Surface chemistry of activated carbons and its characterization. In *Activated Carbon Surfaces in Environmental Remediation*, T. J. Bandosz (ed.), Academic Press, New York, 159–229 (2006).

88. H. P. Boehm, Some aspects of the surface chemistry of carbon blacks and other carbons, *Carbon N. Y.* **32**(5), 759–769 (1994).

89. M. V. Lopez-Ramon, F. Stoeckli, C. Moreno-Castilla, and F. Carrasco-Marin, On the characterization of acidic and basic surface sites on carbons by various techniques, *Carbon N. Y.* **37**(8), 1215–1221 (1999).

90. M. Domingo-García, F. J. López-Garzón, and M. Pérez-Mendoza, Effect of some oxidation treatments on the textural characteristics and surface chemical nature of an activated carbon, *J. Colloid Interface Sci.* **222**(2), 233–240 (2000).

91. I. I. Salame and T. J. Bandosz, Surface chemistry of activated carbons: Combining the results of temperature-programmed desorption, Boehm, and potentiometric titrations, *J Colloid Interface Sci.* **240**(1), 252–258 (2001).

92. M. A. Montes-Morán, D. Suárez, J. A. Menéndez, and E. Fuente, On the nature of basic sites on carbon surfaces: An overview, *Carbon N. Y.* **42**(7), 1219–1225 (2004).

93. Y. El-Sayed and T. J. Bandosz, Adsorption of valeric acid from aqueous solution onto activated carbons: Role of surface basic sites, *J. Colloid Interface Sci.* **273**(1), 64–72 (2004).

94. O. Sirichote, W. Innajitara, and L. Chuenchom, Adsorption of iron (III) ion on activated carbons obtained from bagasse, pericarp of rubber fruit and coconut shell, *Songklanakarin J. Sci. Technol.* **24**, 235–242 (2002).

95. R. C. Bansal and M. Goyal, *Activated Carbon Adsorption*, CRC Press, Boca Raton (2005).

96. J. T. Cookson, Adsorption mechanisms: The chemistry of organic adsorption on activated carbon. In

Carbon Adsorption Handbook, P. N. Cheremisinoff and F. Ellerbusch, Ann Arbor Science, Ann Arbor, 241–279 (1978).

97. V. Gómez-Serrano, M. Acedo-Ramos, A. J. López-Peinado, and C. Valenzuela-Calahorro, Oxidation of activated carbon by hydrogen peroxide. Study of surface functional groups by FT-i.r, *Fuel*. **73**, 387–395 (1994).

98. V. Gómez-Serrano, F. Piriz-Almeida, C. J. Durán-Valle, and J. Pastor-Villegas, Formation of oxygen structures by air activation. A study by FT-IR spectroscopy, *Carbon N. Y.* **37**(10), 1517–1528 (1999).

99. H. Valdés, M. Sánchez-Polo, J. Rivera-Utrilla, and C. A. Zaror, Effect of ozone treatment on surface properties of activated carbon, *Langmuir*. **18**(6), 2111–2116 (2002).

100. H. Tamon and M. Okazaki, Influence of acidic surface oxides of activated carbons on gas adsorption characteristics, *Carbon N. Y.* **34**(6), 741–746 (1996).

101. V. Gómez-Serrano, M. Acedo-Ramos, A. J. López-Peinado, and C. Valenzuela- Calahorro, Mass and surface changes of activated carbon treated with nitric acid. Thermal behavior of the samples, *Thermochim. Acta*. **291**(1-2), 109–115 (1997).

102. C. Moreno-Castilla, M. V. López-Ramón, and F. Carrasco-Marín, Changes in surface chemistry of activated carbons by wet oxidation, *Carbon N. Y.* **38**(14), 1995–2001 (2000).

103. J. Jaramillo, P. M. Álvarez, and V. Gómez-Serrano, Oxidation of activated carbon by dry and wet methods. Surface chemistry and textural modifications, *Fuel Process. Technol.* **91**(11), 1768–1775 (2010).

104. T. J. Bandosz, Surface chemistry of carbon materials. In *Carbon Materials for Catalysis*, P. Serp and J. L. Figueiredo (eds.), Wiley, Hoboken, 45–92 (2009).

105. T. J. Bandosz, J. Jagiello, and J. A. Schwarz, Comparison of methods to assess surface acidic groups on activated carbons, *Anal. Chem.* **64**(8), 891–895 (1992).

106. M. S. Shafeeyan, W. M. A. W. Daud, A. Houshmand, and A. Shamiri, A review on surface modification of activated carbon for carbon dioxide adsorption, *J. Anal. Appl. Pyrolysis*. **89**(2), 143–151 (2010).

107. J. S. Noh and J. A. Schwarz, Effect of HNO3 treatment on the surface acidity of activated carbons, *Carbon N. Y.* **28**(5), 675–682 (1990).

108. Y. Otake and R. G. Jenkins, Characterization of oxygen-containing surface complexes created on a microporous carbon by air and nitric acid treatment, *Carbon N. Y.* **31**(1), 109–121 (1993).

109. J. L. Figueiredo, M. F. R. Pereira, M. M. A. Freitas, and J. J. M. Órfão, Modification of the surface chemistry of activated carbons, *Carbon N. Y.* **37**(9), 1379–1389 (1999).

110. J. F. Vivo-Vilches, E. Bailón-García, A. F. Pérez-Cadenas, F. Carrasco-Marín, and F. J. Maldonado-Hódar, Tailoring the surface chemistry and porosity of activated carbons: Evidence of reorganization and mobility of oxygenated surface groups, *Carbon N. Y.* **68**, 520–530 (2014).

111. C. Moreno-Castilla, M. A. Ferro-Garcia, J. P. Joly, I. Bautista-Toledo, F. Carrasco-Marin, and J. Rivera-Utrilla, Activated carbon surface modifications by nitric acid, hydrogen peroxide, and ammonium peroxydisulfate treatments, *Langmuir*. **11**(11), 4386–4392 (1995).

112. G. S. Szymański, Z. Karpiński, S. Biniak, and A. Świa̧Tkowski, The effect of the gradual thermal decomposition of surface oxygen species on the chemical and catalytic properties of oxidized activated carbon, *Carbon N. Y.* **40**(14), 2627–2639 (2002).

113. J. A. Menéndez, M. J. Illán-Gómez, C. A. L. y León, and L. R. Radovic, On the difference between the isoelectric point and the point of zero charge of carbons, *Carbon N. Y.* **33**(11), 1655–1657 (1995).

114. J. A. Menéndez, J. Phillips, B. Xia, and L. R. Radovic, On the modification and characterization of chemical surface properties of activated carbon: In the search of carbons with stable basic properties, *Langmuir*. **12**(18), 4404–4410 (1996).

115. S. Shin, J. Jang, S.-H. Yoon, and I. Mochida, A study on the effect of heat treatment on functional groups of pitch based activated carbon fiber using FTIR, *Carbon N. Y.* **35**(12), 1739–1743 (1997).

116. J. A. Menéndez, B. Xia, J. Phillips, and L. R. Radovic, On the modification and characterization of chemical surface properties of activated carbon: Microcalorimetric, electrochemical, and thermal desorption probes, *Langmuir*. **13**(13), 3414–3421 (1997).

117. S. A. Dastgheib and T. Karanfil, Adsorption of oxygen by heat-treated granular and fibrous activated carbons, *J. Colloid Interface Sci.* **274**(1), 1–8 (2004).

118. E. Papirer, S. Li, and J.-B. Donnet, Contribution to the study of basic surface groups on carbons, *Carbon N. Y.* **25**(2), 243–247 (1987).

119. U. Zielke, K. J. Hüttinger, and W. P. Hoffman, Surface-oxidized carbon fibers: I. Surface structure and chemistry, *Carbon N. Y.* **34**(8), 983–998 (1996).

120. W. W. Smeltzer and R. McIntosh, The effect of physical adsorption on the electrical resistance of active carbon, *Can. J. Chem.* **31**(12), 1239–1251 (1953).

121. S. S. Barton and J. E. Koresh, A study of the surface oxides on carbon cloth by electrical conductivity, *Carbon N. Y.* **22**(6), 481–485 (1984).

122. A. Barroso-Bogeat, M. Alexandre-Franco, C. Fernández-González, and V. Gómez-Serrano, Preparation of activated carbon-metal (hydr)oxide materials by thermal methods. Thermogravimetric-mass spectrometric (TG-MS) analysis, *J. Anal. Appl. Pyrolysis*. **116**, 243–252 (2015).

123. M. Polovina, B. Babić, B. Kaluderović, and A. Dekanski, Surface characterization of oxidized activated carbon cloth, *Carbon N. Y.* **35**(8), 1047–1052 (1997).

124. Z. Hashisho, M. J. Rood, S. Barot, and J. Bernhard, Role of functional groups on the microwave attenuation and electric resistivity of activated carbon fiber cloth, *Carbon N. Y.* **47**(7), 1814–1823 (2009).

125. D. D. L. Chung, *Applied Materials Science: Applications of Engineering Materials in Structural, Electronics, Thermal, and Other Industries*, CRC Press, Boca Raton (2001).

126. H.-P. Boehm, Catalytic properties of nitrogen-containing carbons. In *Carbon Materials for Catalysis*, P. Serp and J. L. Figueiredo (eds.), Wiley, Hoboken, 219–265 (2009).

127. S. Biniak, G. Szymański, J. Siedlewski, and A. Świątkowski, The characterization of activated carbons with oxygen and nitrogen surface groups, *Carbon N. Y.* **35**(12), 1799–1810 (1997).

128. J. Lahaye, G. Nansé, A. Bagreev, and V. Strelko, Porous structure and surface chemistry of nitrogen containing carbons from polymers, *Carbon N. Y.* **37**(4), 585–590 (1999).

129. N. Inagaki, K. Narushima, H. Hashimoto, and K. Tamura, Implantation of amino functionality into amorphous carbon sheet surfaces by NH3 plasma, *Carbon N. Y.* **45**(4), 797–804 (2007).

130. Y. El-Sayed and T. J. Bandosz, Role of surface oxygen groups in incorporation of nitrogen to activated carbons via ethylmethylamine adsorption, *Langmuir.* **21**(4), 1282–1289 (2005).

131. A. Bagreev, J. A. Menendez, I. Dukhno, Y. Tarasenko, and T. J. Bandosz, Oxidative adsorption of methyl mercaptan on nitrorgen-enriched bituminous coal-based activated carbon, *Carbon N. Y.* **43**(1), 208–210 (2005).

132. M. H. Kasnejad, A. Esfandiari, T. Kaghazchi, and N. Asasian, Effect of pre-oxidation for introduction of nitrogen containing functional groups into the structure of activated carbons and its influence on Cu (II) adsorption, *J. Taiwan Inst. Chem. Eng.* **43**(5), 736–740 (2012).

133. R. J. J. Jansen and H. van Bekkum, XPS of nitrogen-containing functional groups on activated carbon, *Carbon N. Y.* **33**(8), 1021–1027 (1995).

134. R. J. J. Jansen and H. van Bekkum, Amination and ammoxidation of activated carbons, *Carbon N. Y.* **32**(8), 1507–1516 (1994).

135. F. Kapteijn, J. A. Moulijn, S. Matzner, and H.-P. Boehm, The development of nitrogen functionality in model chars during gasification in CO2 and O2, *Carbon N. Y.* **37**(7), 1143–1150 (1999).

136. Y. El-Sayed and T. J. Bandosz, Acetaldehyde adsorption on nitrogen-containing activated carbons, *Langmuir.* **18**(8), 3213–3218 (2002).

137. G. Sethia and A. Sayari, Comprehensive study of ultra-microporous nitrogen-doped activated carbon for CO2 capture, *Carbon N. Y.* **93**, 68–80 (2015).

138. J. Kou and L.-B. Sun, Fabrication of nitrogen-doped porous carbons for highly efficient CO2 capture: Rational choice of a polymer precursor, *J. Mater. Chem. A* . **4**(44), 17299–17307 (2016).

139. J. Fujiki and K. Yogo, The increased CO2 adsorption performance of chitosan-derived activated carbons with nitrogen-doping, *Chem. Commun.* **52**(1), 186–189 (2016).

140. M. Machida, T. Goto, Y. Amano, and T. Iida, Adsorptive removal of nitrate from aqueous solution using nitrogen doped activated carbon, *Chem. Pharm. Bull.* **64**(11), 1555–1559 (2016).

141. Y. Kang, Z. Guo, J. Zhang, H. Xie, H. Liu, and C. Zhang, Enhancement of Ni(II) removal by urea-modified activated carbon derived from Pennisetum alopecuroides with phosphoric acid activation, *J. Taiwan Inst. Chem. Eng.* **60**, 335–341 (2016).

142. Q. Liu, M. Ke, F. Liu, P. Yu, H. Hu, and C. Li, High-performance removal of methyl mercaptan by nitrogen-rich coconut shell activated carbon, *RSC Adv.* **7**(37), 22892–22899 (2017).

143. I. Mochida, Y. Korai, M. Shirahama, S. Kawano, T. Hada, Y. Seo, M. Yoshikawa, and A. Yasutake, Removal of SOx and NOx over activated carbon fibers, *Carbon N. Y.* **38**(2), 227–239 (2000).

144. C.-M. Yang and K. Kaneko, Nitrogen-doped activated carbon fiber as an applicant for NO adsorbent, *J. Colloid Interface Sci.* **255**(2), 236–240 (2002).

145. A. Bagreev, S. Bashkova, and T. J. Bandosz, Adsorption of SO2 on activated carbons: The effect of nitrogen functionality and pore sizes, *Langmuir.* **18**(4), 1257–1264 (2002).

146. A. Bagreev, J. Angel Menendez, I. Dukhno, Y. Tarasenko, and T. J. Bandosz, Bituminous coal-based activated carbons modified with nitrogen as adsorbents of hydrogen sulfide, *Carbon N. Y.* **42**(3), 469–476 (2004).

147. L. Yang, S. Wu, and J. P. Chen, Modification of activated carbon by polyaniline for enhanced adsorption of aqueous arsenate, *Ind. Eng. Chem. Res.* **46**(7), 2133–2140 (2007).

148. M. Hofman and R. Pietrzak, Nitrogen-doped carbonaceous materials for removal of phenol from aqueous solutions, *Sci. World J.* **2012**, 1–8 (0212).

149. G. Yang, H. Chen, H. Qin, and Y. Feng, Amination of activated carbon for enhancing phenol adsorption: Effect of nitrogen-containing functional groups, *Appl. Surf. Sci.* **293**, 299–305 (2014).

150. B. Stöhr, H. P. Boehm, and R. Schlögl, Enhancement of the catalytic activity of activated carbons in oxidation reactions by thermal treatment with ammonia or hydrogen cyanide and observation of a superoxide species as a possible intermediate, *Carbon N. Y.* **29**(6), 707–720 (1991).

151. S.-I. Fujita, K. Yamada, A. Katagiri, H. Watanabe, H. Yoshida, and M. Arai, Nitrogen-doped metal-free carbon catalysts for aerobic oxidation of xanthene, *Appl. Catal. A Gen.* **488**, 171–175 (2014).

152. X. Wang, B. Dai, Y. Wang, and F. Yu, Nitrogen-doped pitch-based spherical active carbon as a non-metal catalyst for acetylene hydrochlorination, *ChemCatChem.* **6**(8), 2339–2344 (2014).

153. B. Zhang, Z. Wen, S. Ci, S. Mao, J. Chen, and Z. He, Synthesizing nitrogen-doped activated carbon and probing its active sites for oxygen reduction reaction in microbial fuel cells, *ACS Appl. Mater. Interfaces.* **6**(10), 7464–7470 (2014).

154. O. Y. Podyacheva and Z. R. Ismagilov, Nitrogen-doped carbon nanomaterials: To the mechanism of growth, electrical conductivity and application in catalysis, *Catal. Today.* **249**, 12–22 (2015).

155. S. Fujita, S. Asano, and M. Arai, Nitrobenzene-assisted reduction of phenylacetylene with hydrazine over nitrogen-doped metal-free activated carbon catalyst: Significance of interactions among substrates and catalyst, *J. Mol. Catal. A Chem.* **423**, 181–184 (2016).

156. T. Tanabe, Y. Yamada, J. Kim, M. Koinuma, S. Kubo, N. Shimano, and S. Sato, Knoevenagel condensation using nitrogen-doped carbon catalysts, *Carbon N. Y.* **109**, 208–220 (2016).

157. H. Tang, B. Xu, M. Xiang, X. Chen, Y. Wang, and Z. Liu, Catalytic performance of nitrogen-doped activated carbon supported Pd catalyst for hydrodechlorination of 2,4-dichlorophenol or chloropentafluoroethane, *Molecules.* **24**(4), 674 (2019).

158. A. Volperts, A. Plavniece, G. Dobele, A. Zhurinsh, I. Kruusenberg, K. Kaare, J. Locs, L. Tamasauskaite-Tamasiunaite, and E. Norkus, Biomass based activated carbons for fuel cells, *Renew. Energy.* **141**, 40–45 (2019).

159. M. Yang and Z. Zhou, Recent breakthroughs in supercapacitors boosted by nitrogen-rich porous carbon materials, *Adv. Sci.* **4**(8), 1600408 (2017).

160. M. Seredych, D. Hulicova-Jurcakova, G. Q. Lu, and T. J. Bandosz, Surface functional groups of carbons and the effects of their chemical character, density and accessibility to ions on electrochemical performance, *Carbon N. Y.* **46**(11), 1475–1488 (2008).

161. T. Cordero-Lanzac, J. M. Rosas, F. J. García-Mateos, J. J. Ternero-Hidalgo, J. Palomo, J. Rodríguez-Mirasol, and T. Cordero, Role of different nitrogen functionalities on the electrochemical performance of activated carbons, *Carbon N. Y.* **126**, 65–76 (2018).

162. V. V. Strelko, V. S. Kuts, and P. A. Thrower, On the mechanism of possible influence of heteroatoms of nitrogen, boron and phosphorus in a carbon matrix on the catalytic activity of carbons in electron transfer reactions, *Carbon N. Y.* **38**(10), 1499–1503 (2000).

163. M. J. Mostazo-López, R. Ruiz-Rosas, E. Morallón, and D. Cazorla-Amorós, Generation of nitrogen functionalities on activated carbons by amidation reactions and Hofmann rearrangement: Chemical and electrochemical characterization, *Carbon N. Y.* **91**, 252–265 (2015).

164. D. Hulicova-Jurcakova, M. Kodama, S. Shiraishi, H. Hatori, Z. H. Zhu, and G. Q. Lu, Nitrogen-enriched nonporous carbon electrodes with extraordinary supercapacitance, *Adv. Funct. Mater.* **19**(11), 1800–1809 (2009).

165. Z. R. Ismagilov, A. E. Shalagina, O. Y. Podyacheva, A. V. Ischenko, L. S. Kibis, A. I. Boronin, Y. A. Chesalov, D. I. Kochubey, A. I. Romanenko, O. B. Anikeeva, T. I. Buryakov, and E. N. Tkachev, Structure and electrical conductivity of nitrogen-doped carbon nanofibers, *Carbon N. Y.* **47**(8), 1922–1929 (2009).

166. J. D. Wiggins-Camacho and K. J. Stevenson, Effect of nitrogen concentration on capacitance, density of states, electronic conductivity, and morphology of N-doped carbon nanotube electrodes, *J. Phys. Chem. C.* **113**(44), 19082–19090 (2009).

167. E. M. M. Ibrahim, V. O. Khavrus, A. Leonhardt, S. Hampel, S. Oswald, M. H. Rümmeli, and B. Büchner, Synthesis, characterization, and electrical properties of nitrogen-doped single-walled carbon nanotubes with different nitrogen content, *Diam. Relat. Mater.* **19**(10), 1199–1206 (2010).

168. M. A. Kanygin, O. V. Sedelnikova, I. P. Asanov, L. G. Bulusheva, A. V. Okotrub, P. P. Kuzhir, A. O. Plyushch, S. A. Maksimenko, K. N. Lapko, A. A. Sokol, O. A. Ivashkevich, and P. Lambin, Effect of nitrogen doping on the electromagnetic properties of carbon nanotube-based composites, *J. Appl. Phys.* **113**(14), 144315 (2013).

169. H. Chen, F. Sun, J. Wang, W. Li, W. Qiao, L. Ling, and D. Long, Nitrogen doping effects on the physical and chemical properties of mesoporous carbons, *J. Phys. Chem. C.* **117**(16), 8318–8328 (1320).

170. D. P. Kim, C. L. Lin, T. Mihalisin, P. Heiney, and M. M. Labes, Electronic properties of nitrogen-doped graphite flakes, *Chem. Mater.* **3**(4), 686–692 (1991).

171. E. Pollak, G. Salitra, A. Soffer, and D. Aurbach, On the reaction of oxygen with nitrogen-containing and nitrogen-free carbons, *Carbon N. Y.* **44**(15), 3302–3307 (2006).

172. W. Shen and W. Fan, Nitrogen-containing porous carbons: Synthesis and application, *J. Mater. Chem. A.* **1**(4), 999–1013 (2013).

173. L. Zhao, N. Baccile, S. Gross, Y. Zhang, W. Wei, Y. Sun, M. Antonietti, and M.-M. Titirici, Sustainable nitrogen-doped carbonaceous materials from biomass derivatives, *Carbon N. Y.* **48**(13), 3778–3787 (2010).

174. M. J. Mostazo-López, R. Ruiz-Rosas, E. Morallón, and D. Cazorla-Amorós, Nitrogen doped superporous carbon prepared by a mild method. Enhancement of supercapacitor performance, *Int. J. Hydrogen Energy.* **41**(43), 19691–19701 (2016).

175. J. Kim, J. Chun, S.-G. Kim, H. Ahn, and K. C. Roh, Nitrogen and fluorine co-doped activated carbon for supercapacitors, *J. Electrochem. Sci. Technol.* **8**(4), 338–343 (2017).

176. M. E. Ramos, J. D. González, P. R. Bonelli, and A. L. Cukierman, Effect of process conditions on physicochemical and electrical characteristics of denim-based activated carbon cloths, *Ind. Eng. Chem. Res.* **46**(4), 1167–1173 (2007).

177. M. E. Ramos, P. R. Bonelli, and A. L. Cukierman, Physico-chemical and electrical properties of activated carbon cloths. Effect of inherent nature of the fabric precursor, *Colloids Surfaces A Physicochem. Eng. Asp.* **324**(1-3), 86–92 (2008).

178. M. E. Ramos, P. R. Bonelli, S. Blacher, M. M. L. Ribeiro Carrott, P. J. M. Carrott, and A. L. Cukierman, Effect of the activating agent on physico-chemical and electrical properties of activated carbon cloths developed from a novel cellulosic precursor, *Colloids Surfaces A Physicochem. Eng. Asp.* **378**(1-3), 87–93 (2011).

179. A. Subrenat, J. N. Baléo, P. Le Cloirec, and P. E. Blanc, Electrical behaviour of activated carbon cloth

heated by the joule effect: Desorption application, *Carbon N. Y.* **39**(5), 707–716 (2001).

180. A. S. Subrenat and P. A. Le Cloirec, Volatile organic compound (VOC) removal by adsorption onto activated carbon fiber cloth and electrothermal desorption: An industrial application, *Chem. Eng. Commun.* **193**(4), 478–486 (2006).

181. K. Nishimiya, T. Hata, H. Kikuchi, and Y. Imamura, Effect of aluminum compound addition on graphitization of wood charcoal by direct electric pulse heating method, *J. Wood Sci.* **50**(2), 177–181 (2004).

182. O. Ioannidou and A. Zabaniotou, Agricultural residues as precursors for activated carbon production-A review, *Renew. Sustain. Energy Rev.* **11**(9), 1966–2005 (2007).

183. H. Marsh, ed., *Introduction to Carbon Science*, Butterworth-Heinemann, Oxford (1989).

184. H. Marsh and F. Rodríguez-Reinoso, *Sciences of Carbon Materials*, Publicaciones de la Universidad de Alicante, Alicante (2000).

185. M. Inagaki and L. R. Radovic, Nanocarbons, *Carbon N. Y.* **40**(12), 2279–2282 (2002).

186. Y.-R. Rhim, D. Zhang, D. H. Fairbrother, K. A. Wepasnick, K. J. Livi, R. J. Bodnar, and D. C. Nagle, Changes in electrical and microstructural properties of microcrystalline cellulose as function of carbonization temperature, *Carbon N. Y.* **48**(4), 1012–1024 (2010).

187. H. Sugimoto and M. Norimoto, Dielectric relaxation due to interfacial polarization for heat-treated wood, *Carbon N. Y.* **42**(1), 211–218 (2004).

188. H. Sugimoto and M. Norimoto, Dielectric relaxation due to the heterogeneous structure of wood charcoal, *J. Wood Sci.* **51**(6), 554–558 (2005).

189. A. K. Kercher and D. C. Nagle, Evaluation of carbonized medium-density fiberboard for electrical applications, *Carbon N. Y.* **40**(8), 1321–1330 (2002).

190. A. K. Kercher and D. C. Nagle, AC electrical measurements support microstructure model for carbonization: A comment on 'dielectric relaxation due to interfacial polarization for heat-treated wood', *Carbon N. Y.* **42**(1), 219–221 (2004).

191. G. Xiao, R. Xiao, B. Jin, W. Zuo, J. Liu, and J. R. Grace, Study on electrical resistivity of rice straw charcoal, *J. Biobased Mat. Bioenergy.* **4**(4), 426–429 (2010).

192. N. Indayaningsih, A. Zulfia, D. Priadi, and S. Hendrana, Study of the electrical conductivity of oil palm fiber carbon, *Adv Mater. Res.* **277**, 137–142 (2011).

193. G. Xiao, W. Xu, Z. Luo, and H. Pang, Characteristics of toluene decomposition and adsorbent regeneration based on electrically conductive charcoal particle-triggered discharge, *RSC Adv.* **7**(71), 44696–44705 (2017).

194. Z.-H. Jiang, D.-S. Zhang, and B.-H. Fei, Effects of carbonization temperature on the microstructure and electrical conductivity of bamboo charcoal, *New Carbon Mater.* **19**, 249–253 (2004).

195. G. Xiao, M. Ni, R. Xiao, X. Gao, and K. Cen, Catalytic carbonization of lignin for production of electrically conductive charcoal, *J. Biobased Mat. Bioenergy.* **6**(1), 69–74 (2012).

196. X. Xu, G. Xiao, and J. Cao, Raman analysis of lignin conductive char, *J. Wuhan Univ. Technol-Mat. Sci. Edit.* **43**, 115–119 (2013).

197. R.-B. Wu, G. Xiao, D. Chen, H.-L. Zhou, M.-J. Ni, X. Gao, and K.-F. Cen, Characteristics of electrically conductive charcoal prepared by high temperature carbonization of lignin, *J. Zhejiang Univ. (Eng. Sci.).* **48**, 1752–1757 (2014).

198. H. Zhou, G. Xiao, R. Wu, L. Huang, M. Ni, X. Gao, and K. Cen, Influence of temperature on the structure of lignin conductive charcoal graphitization, *J. Zhejiang Univ. (Eng. Sci.).* **48**, 2066–2071 (2014).

199. M. Kumar and R. C. Gupta, Electrical resistivity of Acacia and Eucalyptus wood chars, *J. Mater. Sci.* **28**(2), 440–444 (1993).

200. S.-Y. Wang and C.-P. Hung, Electromagnetic shielding efficiency of the electric field of charcoal from six wood species, *J. Wood Sci.* **49**(5), 450–454 (2003).

201. T. Manabe, M. Ohata, S. Yoshizawa, D. Nakajima, S. Goto, K. Uchida, and H. Yajima, Effect of carbonization temperature on the physicochemical structure of wood charcoal, *Trans. Mater. Res. Soc. Japan.* **32**, 1035–1038 (2007).

202. L. S. Parfen'eva, T. S. Orlova, N. F. Kartenko, B. I. Smirnov, I. A. Smirnov, H. Misiorek, A. Jezowski, J. Muha, and M. C. Vera, Structure, electrical resistivity, and thermal conductivity of beech wood biocarbon produced at carbonization temperatures below 1000 °C, *Phys. Solid State .* **53**, 2398–2407 (2011).

203. J. H. Kwon, S. B. Park, N. Ayrilmis, S. W. Oh, and N. H. Kim, Effect of carbonization temperature on electrical resistivity and physical properties of wood and wood-based composites, *Compos. Part B Eng.* **46**, 102–107 (2013).

204. S. Mrozowski, Semiconductivity and diamagnetism of polycrystalline graphite and condensed ring systems, *Phys. Rev.* **85**(4), 609–620 (1952).

205. A. K. Kercher and D. C. Nagle, Microstructural evolution during charcoal carbonization by X-ray diffraction analysis, *Carbon N. Y.* **41**(1), 15–27 (2003).

206. O. Paris, C. Zollfrank, and G. A. Zickler, Decomposition and carbonisation of wood biopolymers–A microstructural study of softwood pyrolysis, *Carbon N. Y.* **43**(1), 53–66 (2005).

207. S. Mrozowski, Electronic properties and band model of carbons, *Carbon N. Y.* **9**(2), 97–109 (1971).

208. K. Nishimiya, T. Hata, Y. Imamura, and S. Ishihara, Analysis of chemical structure of wood charcoal by X-ray photoelectron spectroscopy, *J. Wood Sci.* **44**(1), 56–61 (1998).

209. W. Djeridi, A. Ouederni, N. B. Mansour, P. L. Llewellyn, A. Alyamani, and L. El Mir, Effect of the both texture and electrical properties of activated carbon on the CO2 adsorption capacity, *Mater. Res. Bull.* **73**, 130–139 (2016).

210. M. Weber and M. R. Kamal, Estimation of the volume resistivity of electrically conductive composites, *Polym. Compos.* **18**(6), 711–725 (1997).

211. C. Rodriguez Correa, T. Otto, and A. Kruse, Influence of the biomass components on the pore

formation of activated carbon, *Biomass Bioenergy*. **97**, 53–64 (2017).

212. M. A. Naeem, M. Khalid, M. Arshad, and R. Ahmad, Yield and nutrient composition of biochar produced from different feedstocks at varying pyrolytic temperatures, *Pakistan J. Agric. Sci.* **51**, 75–82 (2014).

213. S. Biniak, A. Świątkowski, and M. Pakuła, Electrochemical studies of phenomena at active carbon-electrolyte solution interfaces. In *Chemistry and Physics of Carbon*, L. R. Radovic (ed.), Marcel Dekker, New York, 27, 125-225 (2001).

214. L. R. Radovic, *Chemistry and Physics of Carbon*, Marcel Dekker, New York, 24 (1994).

215. C. P. Suhas and C. M. Ribeiro, Lignin - from natural adsorbent to activated carbon: A review, *Bioresour. Technol.* **98**, 2301–2312 (2007).

216. A. Jain, R. Balasubramanian, and M. P. Srinivasan, Hydrothermal conversion of biomass waste to activated carbon with high porosity: A review, *Chem. Eng. J.* **283**, 789–805 (2016).

217. M.-M. Titirici, R. J. White, C. Falco, and M. Sevilla, Black perspectives for a green future: Hydrothermal carbons for environment protection and energy storage, *Energy Environ. Sci.* **5**(5), 6796–6822 (2012).

218. K. K. Lee, E. Björkman, D. Morin, M. Lilliestråle, F. Björefors, A. M. Andersson, and N. Hedin, Effects of hydrothermal carbonization conditions on the textural and electrical properties of activated carbons, *Carbon N. Y.* **107**, 619–621 (2016).

219. M. Kurniati, D. Nurhayati, and A. Maddu, Study of structural and electrical conductivity of sugarcane bagasse-carbon with hydrothermal carbonization, *IOP Conf. Ser. Earth Environ. Sci.* **58**, 012049 (2017).

220. K. Siebel, Über die Änderung des elektrischen Widerstandes von Kohle durch Gasabsorption, *Z Physik.* **4**(2), 288–299 (1921).

221. J. W. McBain, *Sorption of Gases and Vapours by Solids*, G. Routledge and Sons, London (1932).

222. G. M. Schwab and B. Karkalos, The electrical conductivity of activated charcoal, *Z. Elektrochem. Angew. Phys. Chem.* **47**, 345–353 (1941).

223. J. Sandor, *The Ultra-Fine Structure of Coals and Cokes*. British Coal Utilization Research Association, London, 342 (1944).

224. J. R. Dacey, G. J. C. Frohnsdorff, and J. T. Gallagher, The effects of adsorbed water on the electrical resistance and the length of Saran charcoal rods-A preliminary account, *Carbon N. Y.* **2**(1), 41–51 (1964).

225. R. McIntosh, R. S. Haines, and G. C. Benson, The effect of physical adsorption on the electrical resistance of activated carbon, *J. Chem. Phys.* **15**(1), 17–27 (1947).

226. S. Brunauer, *The Adsorption of Gases and Vapors*, Princeton University Press, Princeton, 1 (1943).

227. R. A. Beebe, G. L. Kington, M. H. Polley, and W. R. Smith, Heats of adsorption and molecular configuration. The pentanes on carbon black, *J. Am. Chem. Soc.* **72**(1), 40–42 (1950).

228. M. E. Ramos, P. R. Bonelli, A. L. Cukierman, M. M. L. Ribeiro Carrott, and P. J. M. Carrott, Adsorption of volatile organic compounds onto activated carbon cloths derived from a novel regenerated cellulosic precursor, *J. Hazard. Mater.* **177**(1-3), 175–182 (2010).

229. D. L. Johnsen, Z. Zhang, H. Emamipour, Z. Yan, and M. J. Rood, Effect of isobutane adsorption on the electrical resistivity of activated carbon fiber cloth with select physical and chemical properties, *Carbon N. Y.* **76**, 435–445 (2014).

230. N. A. Travlou, M. Seredych, E. Rodríguez-Castellón, and T. J. Bandosz, Activated carbon-based gas sensors: Effects of surface features on the sensing mechanism, *J. Mater. Chem. A.* **3**(7), 3821–3831 (2015).

231. N. A. Travlou, C. Ushay, M. Seredych, E. Rodríguez-Castellón, and T. J. Bandosz, Nitrogen-doped activated carbon-based ammonia sensors: Effect of specific surface functional groups on carbon electronic properties, *ACS Sens.* **1**(5), 591–599 (2016).

232. F. D. Yu, L. Luo, and G. Grevillot, Electrothermal swing adsorption of toluene on an activated carbon monolith. Experiments and parametric theoretical study, *Chem. Eng. Process. Process Intensif.* **46**(1), 70–81 (2007).

233. J. Imai and K. Kaneko, Electrical conductivity of a single micrographitic carbon fiber with a high surface area under various atmospheres, *Langmuir.* **8**(7), 1695–1697 (1992).

234. N. Kobayashi, T. Enoki, C. Ishii, K. Kaneko, and M. Endo, Gas adsorption effects on structural and electrical properties of activated carbon fibers, *J. Chem. Phys.* **109**(5), 1983–1990 (1998).

235. S. L. di Vittorio, M. S. Dresselhaus, M. Endo, J.-P. Issi, L. Piraux, and V. Bayot, The transport properties of activated carbon fibers, *J. Mater. Res.* **6**, 778–783 (1991).

236. M. S. Dresselhaus, A. W. P. Fung, A. M. Rao, S. L. di Vittorio, K. Kuriyama, G. Dresselhaus, and M. Endo, New characterization techniques for activated carbon fibers, *Carbon N. Y.* **30**(7), 1065–1073 (1992).

237. I. S. McLintock and J. C. Orr, The effect of oxygen adsorption on the electrical resistance of evaporated carbon films, *Carbon N. Y.* **6**(3), 309–323 (1968).

238. Y. Shibayama, H. Sato, T. Enoki, M. Endo, and N. Shindo, Magnetic properties of activated carbon fibers and their iodine-doping effect, *Mol. Cryst. Liq. Cryst. Sci. Technol. Sect. A. Mol. Cryst. Liq. Cryst.* **310**(1), 273–278 (1998).

239. M. Kempiński, Resistivity switching in activated carbon fibers, *Mater. Lett.* **230**, 180–182 (2018).

240. A. Barroso-Bogeat, M. Alexandre-Franco, C. Fernández-González, J. Sánchez-González, and V. Gómez-Serrano, Temperature dependence of DC electrical conductivity of activated carbon-metal oxide nanocomposites. Some insight into conduction mechanisms, *J. Phys. Chem. Solids.* **87**, 259–270 (2015).

241. S. Mrozowski, Electric resistivity of polycrystalline graphite and carbons, *Phys. Rev.* **77**(6), 838 (1950).

242. F. Carmona, P. Delhaes, G. Keryer, and J. P. Manceau, Non-metal-metal transition in a non-crystalline carbon, *Solid State Commun.* **14**(11), 1183–1187 (1974).

243. H. Fritzsche, Optical and electrical energy gaps in amorphous semiconductors, *J. Non. Cryst. Solids.* **6**(1), 49–71 (1971).

244. A. C. Metaxas, *Foundations of Electroheat: A Unified Approach*, Wiley, Chichester (1996).

245. R. J. Meredith, *Engineers' Handbook of Industrial Microwave Heating*, The Institution of Electrical Engineers, London (1998).

246. P. D. Sullivan, M. J. Rood, K. J. Hay, and S. Qi, Adsorption and electrothermal desorption of hazardous organic vapors, *J. Environ. Eng.* **127**(3), 217–223 (2001).

247. L. Luo, D. Ramirez, M. J. Rood, G. Grevillot, K. J. Hay, and D. L. Thurston, Adsorption and electrothermal desorption of organic vapors using activated carbon adsorbents with novel morphologies, *Carbon N. Y.* **44**(13), 2715–2723 (2006).

248. A. Nakayama, K. Suzuki, T. Enoki, K-i Koga, M. Endo, and N. Shindo, Electronic and magnetic properties of activated carbon fibers, *Bull. Chem. Soc. Jpn.* **69**(2), 333–339 (1996).

249. A. W. P. Fung, A. M. Rao, K. Kuriyama, M. S. Dresselhaus, G. Dresselhaus, M. Endo, and N. Shindo, Raman scattering and electrical conductivity in highly disordered activated carbon fibers, *J. Mater. Res.* **8**(3), 489–500 (1993).

250. Y. Huang, Electrical and thermal properties of activated carbon fibers. In *Activated Carbon Fiber and Textiles*, J. Y. Chen (ed.), Elsevier Ltd., Cambridge, 181–192 (2017).

251. A. W. P. Fung, M. S. Dresselhaus, and M. Endo, Transport properties near the metal-insulator transition in heat-treated activated carbon fibers, *Phys. Rev. B.* **48**(20), 14953–14962 (1993).

252. M. S. Dresselhaus, G. Dresselhaus, K. Sugihara, I. L. Spain, and H. A. Goldberg, *Graphite Fibers and Filaments*, Springer Verlag, Berlin (1988).

253. A. W. P. Fung, A. M. Rao, K. Kuriyama, M. S. Dresselhaus, G. Dresselhaus, and M. Endo, Characterization of activated carbon fibers. In *Materials Research Society Symposium Proceedings, Volume 209, Defects in Materials*, P. D. Bristowe, J. E. Epperson, J. E. Griffith *et al.* (eds.), Cambridge University Press, New York, 335–340 (1991).

254. A. W. P. Fung, A. M. Rao, K. Kuriyama, M. S. Dresselhaus, G. Dresselhaus, and M. Endo, Transport properties of heat-treated activated carbon fibers. In *Extended Abstracts and Program-Biennial Conference on Carbon*, R. A. Meyer (ed.), American Carbon Society, Santa Barbara, 296–297 (1991).

255. B. Abeles, P. Sheng, M. D. Coutts, and Y. Arie, Structural and electrical properties of granular metal films, *Adv. Phys.* **24**(3), 407–461 (1975).

256. M. Kempiński, W. Kempiński, J. Kaszyński, and M. Śliwińska-Bartkowiak, Model of spin localization in activated carbon fibers, *Appl. Phys. Lett.* **88**(14), 143103 (2006).

257. A. W. Fung, Z. H. Wang, M. S. Dresselhaus, G. Dresselhaus, R. W. Pekala, and M. Endo, Coulomb-gap magnetotransport in granular and porous carbon structures, *Phys. Rev. B Condens. Matter.* **49**(24), 17325–17335 (1994).

258. M. Kempiński, W. Kempiński, and M. Śliwińska-Bartkowiak, Influence of guest molecules adsorption on electronic properties of activated carbon fibers, *Rev. Adv. Mater. Sci.* **12**, 72–77 (2006).

259. I. L. Spain, The electronic transport properties of graphite, carbons, and related materials. In *Chemistry and Physics of Carbon*, P. L. Walker and P. A. Thrower (eds.), Marcel Dekker, New York, 16, 119 (1981).

260. J. Robertson, Amorphous carbon, *Adv. Phys.* **35**(4), 317–374 (1986).

261. B. Kastening, A model of the electronic properties of activated carbon, *Ber. Bunsenges. Phys. Chem.* **102**(2), 229–237 (1998).

262. N. F. Mott and E. A. Davis, *Electronic Processes in Non-Crystalline Materials*, 1st ed., Clarendon Press, Oxford (1971).

263. P. Sheng and J. Klafter, Hopping conductivity in granular disordered systems, *Phys. Rev. B.* **27**(4), 2583–2586 (1983).

264. B. Kastening, M. Hahn, B. Rabanus, M. Heins, and U. Zum Felde, Electronic properties and double layer of activated carbon, *Electrochim. Acta.* **42**(18), 2789–2799 (1997).

265. A. Nakayama, K. Suzuki, T. Enoki, S. L. di Vittorio, M. S. Dresselhaus, K. Koga, M. Endo, and N. Shindo, Magnetic properties of activated carbon fibers, *Synth. Met.* **57**(1), 3736–3741 (1993).

266. S. Lengyel and B. E. Conway, Thermodynamic and transport properties of aqueous and molten electrolytes. In *Comprehensive Treatise of Electrochemistry*, B. E. Conway, J. O Bockris, and E. Yeager (eds.), Plenum Press, New York, 5, 16–47 (1983).